Instrumentation Development, Measurement and Performance Evaluation of Environmental Technologies

Quarterly Technical Progress Report
for the period
July 1, 1999 - September 30, 1999

Dr. John Plodinec, Principal Investigator

Report No. 40395R05

Prepared for the U.S. Department of Energy
Agreement No. DE-FT26-98FT40395

Diagnostic Instrumentation and Analysis Laboratory
Mississippi State University
205 Research Boulevard
Starkville, Mississippi 39759-9734

dial@dial.msstate.edu
www.msstate.edu/Dept/DIAL

Notice

Table of Contents

List of Figures v

List of Tables vii

Executive Summary 1

Task 1. Instrumentation Development 1
Task 2. Measurement Support 2
Task 3. Performance Evaluation 2

TASK 1 Instrumentation Development 5

Air Plasma Off-gas Emission Monitor 6
Detection of Toxic Compounds by Cavity Ring-Down Spectroscopy 27
Volatile Organic Compound Monitoring Using Diode Lasers 28
Laser Induced Fluorescence Spectrometry of Radio-nuclides 33
Cavity Ringdown Monitors for Transuranic Elements . . . 37
Feasibility of Characterizing Solid Wastes by Remotely Sensed Multispectral Images 40
Guided Wave Nondestructive Evaluation Technique Development and Demonstration 43

TASK 2 Measurement Support 49

Diagnostic Field Applications Coordination and Testing Support 49
On-line Imaging for Thermal Treatment Processes 49

TASK 3 Performance Evaluation 50

Dissolution of Hanford Salt 51
Wall Removal Monitor 70
Pipe Decontamination 74
Drum Pressure Monitor 77
Plasma Treatment of VOCs and Other Off-gas Components by Pulsed Micro Hollow Cathode Plasma Array . . 80
Laser-induced Breakdown Spectroscopy 83

List of Figures

FIGURE 1. APO-GEM schematic diagram 8
FIGURE 2. (a) The continuous sampling air-ICP system connected to the combustion test stand at DIAL. Near the top of the photograph, the glass lined sampling probe is shown inserted into a vertical section of the test stand and connected to the black heat traced sample line. (b) The air-ICP sampling probe, inserted into the stack, showing the nebulizer spike location – the white Teflon tee between the probe and the sample line 14
FIGURE 3. Time scan emission monitoring for beryllium (Be (II) 313.04 nm), obtained for the introduction of a 100-ppm Be solution and a water blank, using the ultrasonic nebulizer (stack not connected) 18
FIGURE 4. (a) Time scan monitoring data for chromium (Cr (I) 359.35 nm), with metals introduced into the stack, water introduced into the stack, and Cr calibration spikes added to the sampled gas stream. (b) Calibration curve for Cr, generated from the time scan data 20
FIGURE 5. Time scan calibration spiking data for (a) beryllium (Be (II) 313.11 nm) and (c) lead (Pb (I) 405.78 nm), with metals introduced into the stack, water introduced into the stack, and calibration spikes added to the sampled gas stream. Calibration curves for (b) Be and (d) Pb, generated from the time scan data. 22
FIGURE 6. Time scan monitoring for (a) chromium (Cr (I) 359.35 nm) and (b) beryllium (Be (II) 313.11 nm) during the second RM-29 sampling conducted on September 16. The detector integration time used was 3-s per point 24
FIGURE 7. Experimental configuration for diode laser absorption spectrometry 30
FIGURE 8. Absorbance measurements for benzene in 730 Torr of nitrogen with diode laser temperature set at 35 C . . . 32
FIGURE 9. Absorbance measurements for benzene in 730 Torr of air with diode laser temperature set at 35 C 32

FIGURE 10. Schematic of the laser induced fluorescence spectrometry technique 35
FIGURE 11. Schematic of isotopic energy shifts and the associated LIF spectrum 35
FIGURE 12. Schematic of infrared diffuse reflectance multi-spectral imaging technique (final configuration) 41
FIGURE 13. Comparison of the ESP predictions of nitrate concentration with experimental data of Herting 63
FIGURE 14. Comparison of ESP predictions of sulfate concentration with experimental data of Herting 65
FIGURE 15. Comparison of ESP predictions of TIC concentration with experimental data of Herting 68
FIGURE 16. LIBS experimental setup 85
FIGURE 17. Atomic line intensity at different gas flow rates 85
FIGURE 18. Cr calibration data at different gas temperatures 86

List of Tables

TABLE 1. Detection limits for the APO-GEM for various metals. . 10
TABLE 2. Relative accuracy of DIAL Air-ICP data 11
TABLE 3. Major constituents in saltcakes 55
TABLE 4. Impact of charge reconciliation method on adjusted ion concentrations - Tank BY-106 57
TABLE 5. Impact of charge reconciliation method on generated molecular stream - Tank BY-106 58
TABLE 6. Comparison of predicted percent water with experimental measurements 60
TABLE 7. Atomic line intensity ratios at different gas flow rates . . 86

Executive Summary

The Diagnostic Instrumentation and Analysis Laboratory (DIAL) at Mississippi State University (MSU) will undertake three tasks for DOE EM during the period April 1, 1999 through March 31, 2000.

Task 1. Instrumentation Development

Instrumentation will be developed for unique DOE site needs. Some of the needs identified by the DOE sites require development of new instrumentation, for example, development of continuous emissions monitors for metals, or for dioxins and furans. DIAL, with its rare ability to both develop, adapt, and simulate field service of new instrumentation, is ideally suited for this mission.

Volatile Organic Compound Monitoring Using Diode Lasers. Diode laser absorption spectroscopy was employed to carry out atmospheric pressure measurements of trace quantities of benzene in nitrogen and air. To our knowledge, these are the first measurements of their kind. The results obtained were in excellent agreement with earlier low-pressure absorption measurements and indicated that atmospheric pressure broadening does not negatively impact our ability to measure benzene in air. Preparations are underway to extend these studies to chlorobenzene.

Task 2. Measurement Support

Measurement services will be provided for DOE sites. In some cases, a specific site will not be able to justify the cost of a new instrument but will need it to achieve a programmatic objective. DIAL can take its instrumentation to the DOE site to provide the measurements needed.

Task 3. Performance Evaluation

The performance of environmental technologies will be evaluated for DOE. DOE EM needs a tool which will rapidly, and without bias, allow it to compare the performance of technologies against the field's needs, so that it can focus its development dollars on the highest impact targets. DOE EM also needs a tool to rapidly screen new technologies to assist in the most effective allocation of its development funding. Further, the technology developers (and DOE EM) need a tool to expedite the acceptance of developed technologies into the DOE EM user facilities. DIAL is ideally suited to address both of these needs. Through its network of contacts within the DOE sites, DIAL can rapidly elicit user needs. Through its knowledge of the technologies needed, and its network of contacts in industry, DIAL can rapidly identify promising candidates to satisfy those needs. DIAL's experienced multidisciplinary staff can then provide users with the information they need to make deployment decisions, by using DIAL's wide-ranging measurement capabilities in either its own testing facilities, or in those of its network of collaborators if more appropriate for a given application.

Dissolution of Hanford Salt. Results are presented for the comparison of ESP predictions and experimental results for saltcake compositions from four Hanford tanks. Preprocessing of the data was accomplished through the use of a propation charge reconciliation

method and then tuning the stream composition to the experimentally determined percent water in the samples. Simulations show excellent agreement with the experimental dilution data at both high and low ionic strengths for nitrate, carbonate, and oxalate ions. Results for sulfate and phosphate ions are in good agreement with experimental data when fluoride is absent. In the presence of fluoride, the model predicts the presence of the Na-F-SO_4 and Na-F-PO_4 double salts, and this is confirmed by experiments at the site. The dissolution behavior of the double salts predicted by ESP was not in agreement with the experimental results and work is now in progress to obtain the experimental data for these systems.

Wall Removal Monitor. In support of the DOE's decontamination and decommissioning (D&D) of concrete structures, DIAL has developed a technology for monitoring scabbling operations. To D&D a concrete structure, the thin (~.5 inch) layer of contaminated concrete is removed by a process called scabbling. Current technology requires a surveying crew to measure points on the structure at 1-foot intervals. After the survey is completed the scabbling contractor performs the removal operation, and then the surveying crew comes back to make measurements. This process is time consuming and complicated, and if the contractor does not remove the required amount of material, additional cost and time is required to correct and re-measure the results. The wall removal monitor runs in real time providing information about the amount of material removed while the scabbling operation is occurring. In tests, the system is placed ~30 feet from the wall (well out of the way of operating machinery) and measures 145 square feet at a time. Data collection takes only seconds, and set-up requires only 30 minutes.

Drum Pressure Monitor. Due to the aging of stockpiles of stored waste, especially those in 55-gallon drums, containers are becoming pressurized and are rupturing. Several events have been recorded in the DOE's Operating Experience Weekly Summary by the Office of Nuclear Safety (OEWS 95-02) where drums have ruptured and

spilled hazardous contents or destroyed property (such as overhead light fixtures). A method of detecting drums that are under pressure has been developed at DIAL. The method relates the pressure in the drum to the frequency at which the lid vibrates. We are currently refining our models, establishing detection limits, and searching for commercial partners.

Plasma Treatment of VOCs and Other Off-gas Components by Pulsed Micro-hollow Cathode Plasma Array. Preliminary design work was completed and purchase orders written for the power supply and vacuum components. Additional progress has been delayed due to a lack of manpower.

Laser-induced Breakdown Spectroscopy . Work continued on the study of the effects of gas stream conditions on LIBS measurements. The experiments were conducted in a mini-combustion test stand. LIBS spectra were recorded under different gas flows and gas temperatures. Initial results show the LIBS signal did not following the change of gas density in these measurements. This was later determined to be due to the nonlinear effect of the ultrasonic nebulizer efficiency. The nebulizer cannot efficiently deliver a metal aerosol with a high metal concentration solution. To avoid using a high metal concentration solution in the study, measurements will be repeated with Be which is the most sensitive element in LIBS measurements.

TASK 1 *Instrumentation Development*

Many of the DOE sites require development of new instrumentation, for example, development of continuous emissions monitors for metals, or for dioxins and furans. DIAL is developing or adapting instrumentation to meet field needs. In each case, these instruments are being developed and tested under simulated service conditions to increase the probability of success.

DIAL is developing new instruments, or adapting existing instrumentation, to address DOE needs. This year, development of emissions monitors for metals and for dioxins and furans continues. Development of instrumentation to determine trace levels of actinides in process solutions or groundwater also continues. Development of more compact process monitors using diode lasers has been initiateed. The feasibility of using remote sensing techniques to characterize solid waste, and of a guided wave technique to determine whether a leak exists in a waste tank, is also being determined.

Air Plasma Off-gas Emission Monitor

G. P. Miller

Introduction

Technology Description

Increasing regulatory demands requiring significant reductions in the emission of hazardous air pollutants have led to the need for techniques capable of providing real time monitoring, at the stack, of toxic metals in combustion gas streams. These waste streams range from coal fired boilers, and municipal waste combustors to plasma vitrification systems used for the remediation of low level radioactive waste. This lack of a fieldable continuous emission metal monitor (CEM) and process monitor (PM) has been recognized as a significant gap in the available technology. The system described below has been designed to fill this gap.

Over the last twenty years the use of argon ICP-AES for the measurement of trace elements in solution has matured into a standard analytical technique. However, unlike the laboratory ICP, it is essential for a CEM that the system be hardened sufficiently to handle the problems of a real world environment. These problems include the ability to readily tolerate the introduction of a variety of molecular gas matrices, significant variations in moisture and particle loading as well as the thermal, vibrational and clogging problems found outside the laboratory. The system under development at DIAL has taken the advantages inherent in inductively coupled plasma technology and incorporated them into APO-GEM, a CEM capable of tolerating the real world environment while accurately measuring the real time concentration of metals in exhaust stacks. Although APO-GEM provides significant reduction in operating costs, the main advantages of the air plasma lie in its increased tolerance of molecular gases, particle load-

ing and reduced susceptibility to moisture content (due to more efficient heat transfer from the air plasma to the sample). On the other hand, it requires higher rf powers and the maximum available ionization energy is reduced from that available in an argon plasma.

The introduction of exhaust gases into the air plasma results in a considerably more complex spectra than the line spectra seen in an argon plasma. The emission spectra includes numerous molecular bands (e.g., OH, CN, NO, N_2^+) in the wavelength regions of interest (200 - 350 nm). This increase in interferences places stringent requirements on both the resolution of the detection system and the software used to analyze the data. We are developing two separate approaches to address these problems, a unique chemometric software package to handle the analysis and an ongoing collaboration with Ames National Laboratory to reduce the size of the detection system while increasing the resolution.

The remaining hardware required to complete the system consists of an isokinetic sampling interface between the APO-GEM and the exhaust duct. The extractive sampling techniques used introduce the sample stream into a controlled environment where matrix effects are minimized and the plasma properties are stabilized. Calibration is handled by a unique system which mixes calibration standards with the combustion stream via the isokinetic sampling apparatus. This effectively compensates for any remaining matrix effects, options that are impossible for in-stack methods.

Instrumentation

The APO-GEM system incorporates a novel 3.5-kW solid state 27.12-MHz rf generator with the load coil modified for air plasma operation. This is coupled to a detection system with the off-gas sample being extracted from the duct and introduced into the air plasma via an isokinetic sampling system. Figure 1 is a schematic diagram of the APO-GEM continuous emission monitor.

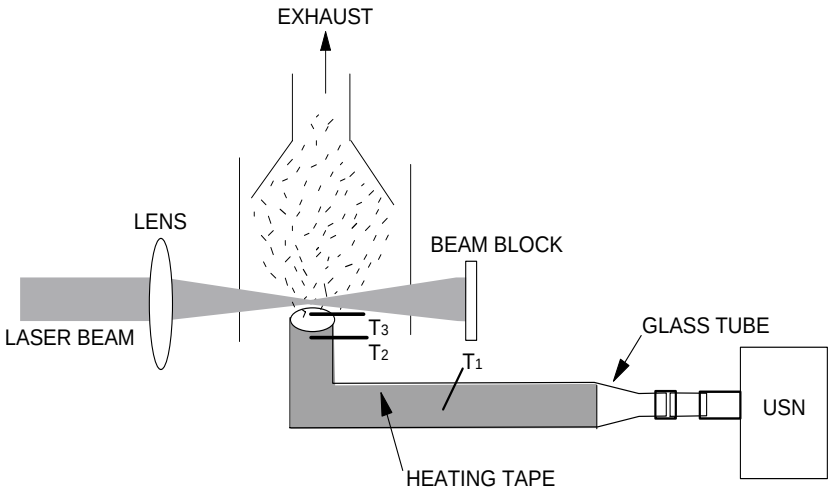

FIGURE 1. APO-GEM schematic diagram.

The APO-GEM plasma is started using argon and progressively switched over to air. Calibration is performed using an ultrasonic nebulizer. The detection system uses a 1-m monochromator, and CCD detector. This remains the largest single component of the system. It has adequate resolution but operates sequentially and is relatively large. It, nevertheless, provides the ideal platform for identifying and characterizing the spectral emissions and possible interferences arising from unidentified components making up exhaust gas emissions. (To provide simultaneous metal concentration measurements, this monochromator could be replaced by a polychromator.) In addition, we are evaluating a novel solid state spectrometer developed for this project by Dr. David Baldwin at Ames National Laboratory. This instrument is compact, thermally and vibrationally stable. It uses a combination of an acousto optic tunable filter and an echelle grating to provide the resolution of a 1.5-m monochromator into a 10-kg package. The successful combination of the solid state APO-GEM and this spectrometer represents a large step forward in instrument development and will reduce the overall size and weight of the com-

plete package substantially (from the original ~1000 kg, to the present 250 kg, then to ~150 kg) while improving the resolution, and thereby the detection limits.

Isokinetic sampling system. To correctly measure the concentration of metals present within an exhaust gas stream it is necessary to introduce a sample from the exhaust gas stream into the ICP under isokinetic conditions. Therefore, a sampling system has been designed to extract such a sample from a gas stream and introduce it into the air plasma for analysis. The system operates by filling a loop with sample gas and then pushing this sample with air into the plasma. The robustness of the air plasma permits an optimum sample flow rate into the ICP of 1.14 sl/min, approximately three times more than tolerated by an argon plasma.

Calibration. An important concern with any CEM is the question of calibration. In this instance, instrument calibration follows a modified standard ICP calibration procedure.[1] An ultrasonic nebulizer is used to provide metal containing aerosols at a known concentration ($\mu g/m^3$). This concentration is determined from

$$C_A = \frac{C_s u \varepsilon}{F} \qquad \textbf{(EQ 1)}$$

where C_A is the aerosol concentration ($x\ 10^3\ \mu g/m^3$), C_s is the standard solution concentration ($\mu g/g_{solv}$), u is the solution uptake to the ultrasonic nebulizer, F is the air flow rate to the plasma, and ε is the nebulizer efficiency. The efficiency of the nebulizer was determined both in the laboratory and again on site prior to the test. For the initial instrument calibration, the metal aerosol was mixed with ambient air. Instrument response was checked against standard calibration curves prepared previously. In the field, the presence of fly ash as well as variations in loading and exhaust gas composition allow the possibility of substantial matrix effects significantly impacting the results of any real world analysis. This variation in composition between laboratory air and the exhaust gas composition renders any direct compar-

ison of the laboratory air calibrations to the instrument off-gas response highly suspect. To circumvent this problem, we have developed a novel technique whereby the calibration standards are mixed with the exhaust off-gas at the entrance to the sampling loop while maintaining isokinetic conditions. This ensures that the standard and off-gas sample are matrix matched. This allows recalibration and QA checks to be performed on-line under actual operating conditions.

To further improve the sensitivity of the instrument, a novel chemometric software package has been developed which, by modeling background spectrum (at the spectra regions of interest), effectively reduces the background noise and thus improves the instrument sensitivity. To apply this method accurately, data from the spectral regions of interest was collected during the shakedown period prior to the test. In addition, as the instrument presently employs a sequential detection system, wavelength calibration is essential. A chemometric based software package was developed to check and, if necessary, correct wavelength calibration. This software checks the wavelength position with respect to the pixel position on the CCD every time the wavelength setting is changed as well as periodically checking for instrument drift.

Detection limits. The toxic metals species of concern to EPA and DOE include As, Be, Cd, Cr, Hg, Sb, and Pb. The present detection limits for a number of metals are given in Table 1. Further improvements in sensitivity are required to meet the expected emission limits.

TABLE 1. Detection limits for the APO-GEM for various metals.

Metal Instrument	Detection Limits (µg/dscm)
As	47
Be	0.07
Cd	2.5
Co	0.6

TABLE 1. Detection limits for the APO-GEM for various metals.

Metal Instrument	Detection Limits (µg/dscm)
Cr	0.25
Hg	20
Mg	0.05
Ni	0.4
Pb	0.9
Sb	55
Sr	0.003

Metal concentrations and relative accuracy. The DOE/EPA demonstration at Raleigh was the first opportunity to check the accuracy and quality of the data provided by the APO-GEM. The relative errors with respect to EPA Method 29 are given in Table 2. Three of the five metals are within 30% for the high concentration level (75 µg/dscm). None are within that range at the low concentration level (15 µg/dscm). These results are excellent considering the uncertainty present in the RM data at these low levels.

TABLE 2. Relative accuracy of DIAL Air-ICP data.

	Be	Cd	Cr	Hg	Pb
RM 1 to 10	40%	26%	40%	13%	21%
RM 11 to 20	43%	46%	59%	67%	42%

Work Accomplished

The present multi metal CEM system under development at DIAL as a source for emissions monitoring utilizes an atmospheric pressure plasma. It has the advantages of being stable and well characterized in terms of plasma properties and possible interferences effects. This method also has the advantages and disadvantages of a

duty cycle. That is, it reduces sampling to twice a minute but maintains stability and reduces the potential of clogging. A system that uses continuous sampling into a reduced pressure ICP increases the sample rate but introduces questions regarding plasma properties, signal stability, and increases clogging potential. Whether the advantage of continuous sampling out weighs these other considerations is being explored by the development of a reduced pressure air-ICP CEM in addition to the discrete sampling system presently used on APO-GEM. This particular configuration was first assembled our collaborators at Ames Laboratory and tested with an ICP power supply and matching network in their laboratory.

The first test of such a system was performed during this quarter at DIAL. The test involve a number of tasks including:

- integration of a compact solid state ICP power supply and its matching network with the reduced pressure plasma system developed at Ames;
- integration of the AOTF-echelle spectrometer with the reduced pressure air-ICP system;
- connection of the reduced pressure air-ICP and continuous sampling system to a sampling port on the DIAL “test stand” (combustion system); and
- operation of the CEM for metals analysis while simultaneously collecting samples using RM-29 for later comparison.

This test was the first field test of the continuous sampling system. While a number of issues arose during this test, all tasks were completed, and a number of significant issues were addressed. Full details regarding the system operations and specifications can be found in Ames Laboratory - USDOE Report IS-5138 “Testing of a Continuous Sampling Air-ICP System as a Continuous Emission Monitor at the Diagnostic Instrumentation and Analysis Laboratory” by D. P. Baldwin, D. S. Zamzow, D. E. Eckels, R. R. Wiser, S. Tao and G. P. Miller.

The test was performed during the week of September 12, 1999, on the combustion test stand at DIAL. This system is a fuel oil air furnace with capabilities for air preheating, introduction of fly ash mixed with the fuel, and introduction of heavy metal aerosols in the exhaust line. Figure 2(a) shows the air-ICP system in front of the scaffolding, connected to the combustion test stand. During the test, the furnace was operated with 227 kg/h of air and 4.5 kg/h of fuel oil, which produced a gas flow in the 8-in. diameter, schedule-80 pipe (19.4-cm inside diameter) of approximately 3000 standard L/min. At the sampling point, the gas temperature was 235˚C, with a velocity of approximately 3.1 m/s. The air-ICP CEM sampling probe was installed in a vertical section of the exhaust line, several meters downstream from the water cooled exhaust line, as shown in Figure 2(b). In order to minimize differences between sample concentrations at various locations in the exhaust line due to drop out of particles and particle segregation, RM-29 sampling occurred at a port in the vertical pipe across from and within a few centimeters of the sampling port for the air-ICP. (To confirm the uniformity of sample concentrations, simultaneous RM-29 measurements were made prior to the test.) At the sampling ports, the exhaust gas was flowing vertically down the pipe. About two meters above the ports, a pneumatic air driven nebulizer at the top of the vertical section introduced appropriate concentrations of aqueous solutions of Be, Cd, Cr, Pb, and Hg into the exhaust gases. During the time that the CEM was collecting data and toxic metals were being introduced into the exhaust stream, samples of the exhaust stream were collected using RM-29. The collected samples have been sent to a certified laboratory for quantitative analysis.

FIGURE 2. **(a) The continuous sampling air-ICP system connected to the combustion test stand at DIAL. Near the top of the photograph, the glass lined sampling probe is shown inserted into a vertical section of the test stand and connected to the black heat traced sample line. (b) The air-ICP sampling probe, inserted into the stack, showing the nebulizer spike location – the white Teflon tee between the probe and the sample line.**

The details of the sampling system for the air-ICP are described in Ref. 1. The temperature of the gases sampled from the exhaust line was 235˚C, which is within the temperature range specification of the EPA isokinetic sampling probe that was used, but was too high for the Teflon sample line. This line transports the gas stream to the Teflon

sampling chamber, from which a secondary sample is drawn for introduction into the ICP torch, inside the reduced pressure enclosure. Although the sampling probe has an integral heater, it was not used. Instead, the sampled gas was allowed to cool to a temperature of 125˚C in the probe before entering the Teflon sample line. From that point, the sample line was electrically heated to maintain a temperature in the range of 105 to 120˚C, to prevent the condensation of water in the sampled gas. For this test, because of the large air to fuel ratio employed at DIAL, the water content of the exhaust gas was only about 5%. A sampling rate from the exhaust pipe of 22 standard L/min was employed. The gas pressure in the test stand at the sampling point was about 1.5 kPa (15 cm of water) below atmospheric pressure. To extract this sample flow from the stack, the plasma enclosure had to be operated at a lower pressure than was used during laboratory testing of the air-ICP system. The Roots blower was operated at a speed of about 2400 rpm and at a pressure of 4.4 kPa (45 cm of water) below ambient atmospheric.

When the air-ICP system was connected to the stack, significant fluctuations in the sample gas flow into the plasma occurred. The reason for the sample flow variation was due to pressure fluctuations in the exhaust pipe, at least 10% variation, on a one-second time scale. The magnitude of these was unexpected, and the sampling system was not able to adequately compensate for this. When the air-ICP system was connected to the stack, a sample flow to the axial channel of the torch corresponding to a differential pressure of approximately 0.3 in. of water was used. However, due to stack flow and pressure variations, the differential pressure indicated by the oil filled manometer varied between approximately 0.25 and 0.35 in. of water, with excursions as low as 0.2 in. and as high as 0.4 in. This large variation in gas flow rate into the axial channel of the air-ICP (from approximately 1.0 to 1.4 L/min) caused obvious fluctuations in the intensity of the plasma during operation of the air-ICP and during collection of data.

Prior to collecting data, the reduced pressure air-ICP system was assembled and integrated into the combustion test stand. This was done primarily during the first two days at DIAL. This initial setup included coupling the reduced pressure plasma enclosure to DIAL's generator and AMN, a compact, solid state, 27-MHz, 3-kW ICP system from Seren Industrial Power Systems. Since this RF generator had not been used with the reduced pressure air-ICP system previously, some time was required to accomplish this task. A number of different load coils for the ICP torch were made and tested for operation of the reduced pressure plasma with the Seren system.

The AOTF-echelle spectrometer, delivered to DIAL in FY 98, was initially incorporated with the reduced pressure plasma system for detecting optical emissions from metals in the sampled gas stream introduced into the air-ICP CEM. After some time spent aligning and trying to optimize signal intensities observed using the AOTF-echelle spectrometer, it became apparent that the AOTF was not functioning correctly. Very low signal intensities were observed for AOTF-selected emission lines, which meant that either the efficiency of the AOTF crystal was much lower than that observed previously, or that the RF power supplied by the AOTF controller was too low. (Preliminary inspection of the AOTF indicated that the AOTF crystal was no longer functioning.) The AOTF was removed and replaced by a 0.2-m focal length monochromator (ISA model H-20) as the prefilter for the echelle spectrometer. Relatively little optimization of the alignment of the echelle spectrometer, using the 0.2-m monochromator, was done due to the time constraints of the testing. Therefore, the limits of detection (LOD) determined for Be, Cd and Hg during the testing are not optimum and are worse than laboratory values obtained previously using the air-ICP.

The continuous sampling air-ICP system was in operation throughout the day (approximately seven hours continuous operation) on September 16. During the day, continuous emission monitoring of metals in the DIAL exhaust stack using the air-ICP CEM system was

performed before, during and after the collection of two RM-29 samples by DIAL personnel, with one sample set collected in the morning and one in the afternoon. Prior to the first RM-29 sample collection, and before the operating air-ICP system was connected to the stack, testing of the air-ICP system for the detection of Be, Cd, Cr, Hg and Pb was performed. This was done by nebulizing solution standards and introducing the dry aerosol into the sample line. This spiked gas stream was sampled using the sampling system, and introduced into the axial channel of the air-ICP. Solution standards of 100 ppm Be, Cd, Cr, and Pb and 1000 ppm Hg were introduced and detected. Spectral data files were acquired and time scan emission monitoring was performed. An example of the time scan monitoring is shown in Figure 3 for Be. The Be (II) 313.04-nm emission signal was detected using a 1-s per point integration time, for the introduction of 100 ppm Be and for a water blank solution. From the signal to noise ratio of the time scan data in Figure 6, a solution concentration limit of detection (LOD) of 0.59 ppm Be is obtained (3-σ standard deviation of the blank definition). Based on the solution flow rate to the ultrasonic nebulizer (1.9 mL/min), the approximate nebulizer efficiency (15%), and the gas flow rates through the nebulizer (1 L/min) and the sampling chamber (22 L/min), the approximate corresponding aerosol LOD is 7.7 µg/dscm for Be. In a similar fashion, detection limits for cadmium (Cd (I) 228.80 nm), chromium (Cr (I) 359.35 nm), mercury (Hg (I) 253.65 nm), and lead (Pb (I) 405.78 nm) were determined for the air-ICP system, without the heat traced sample line connected to the DIAL stack. The solution LODs for Cd, Cr, Hg and Pb were 11.6, 0.092, 52.3 and 0.96 ppm, respectively, which correspond to aerosol concentrations of 150, 1.2, 680 and 12.5 µg/dscm for these four elements. The magnitude of the signal intensity for the 100-ppm Cr solution saturated the CCD detector, for the 1-s integration time used. This fact was not realized during acquisition of the time scan data. As a result, the LOD for Cr is actually lower than the 1.2-µg/dscm value listed above. The LODs for Be, Cd and Hg obtained during the testing at DIAL are worse than the values

obtained previously due to the less than optimum alignment of the 0.2-m monochromator-echelle spectrometer system during the test.

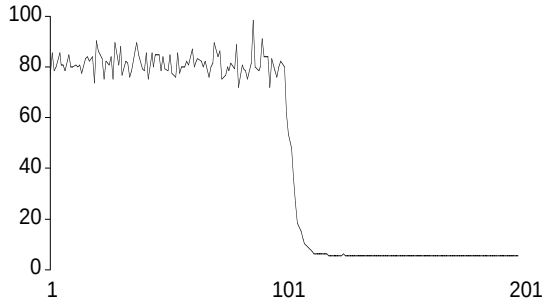

FIGURE 3. Time scan emission monitoring for beryllium (Be (II) 313.04 nm), obtained for the introduction of a 100-ppm Be solution and a water blank, using the ultrasonic nebulizer (stack not connected).

Following these initial experiments, the sample line was connected to the stack and acquisition of the first RM-29 sample was begun. During this time, spectral data acquisition and time scan emission monitoring was performed using the air-ICP and echelle spectrometer system. Time scan monitoring data was collected for Be, Cr and Pb during the RM-29 run. Cadmium and Hg were not detected in the sampled stack gas. Based on the relatively poor detection limits for Cd and Hg above, it is not surprising that these two metals were not detected in the stack gas stream. Due to the significant variations in the sampled gas flow rate into the axial channel of the ICP when the air-ICP sampling system was connected to the stack, only time scan emission monitoring was performed during the RM-29 sampling. Calibration experiments were not conducted because of the significant variation in signal intensities measured for Be, Cr and Pb when the stack was connected. (In retrospect, these calibration experiments could have been done if sufficient time averaging of the signal intensities had been used.) After the first RM-29 sample acquisition was completed, a series of time scan monitoring and calibration spiking experiments were performed for Be, Cr and Pb. The calibration

spiking data for Cr is shown in Figure 4(a). The initial time scan intensity in Figure 4(a), approximately the first 75 s (integration time was 1-s per point), is the signal detected for Cr while metals were being introduced into the stack. After this, the metals solution was replaced with a blank solution (points 75 - 400). From points 400 - 1000, a series of solutions containing increasing concentrations of Cr (5, 10, 50 and 100 ppm) were introduced, using the ultrasonic nebulizer, into the sampled gas stream at the spike location in order to perform on-line calibration. The increase in the signal variation resulting from the sample flow variations that occurred during the testing at DIAL when the air-ICP was connected to the stack is very obvious in Figure 4(a). The signal variation for the signal plateaus in the time scan stack monitoring data was typically in the range of 20 - 60% rsd for Cr, Pb and Be, for 1-s detector integration times. For Cr, the rsd was typically about 20% (Figure 4(a) and other time scan monitoring data not shown). For time scan data acquired when the air-ICP was not connected to the stack (such as that for Be in Figure 3 above), the rsd was in the 3 - 5% range. The calibration curve in Figure 4(b) was generated from the time scan data for Cr, using signal intensities that were averaged over as many time scan data points as possible. The Cr signals measured for the 50- and 100-ppm spikes in Figure 4(a) were suppressed, due to saturation of the CCD detector for the 1-s integration time used. Therefore, for the Cr calibration curve shown in Figure 4(b), these points were not included in the linear regression fit of intensity vs. concentration. The measured Cr intensity corresponds to a solution concentration of 5.7 ppm Cr for the stack metals signal in Figure 4(a), points 1 - 75, using the Cr calibration curve. Based on the solution flow rate to the ultrasonic nebulizer (1.4 mL/min), nebulizer efficiency (15%), the gas flow rates through the nebulizer (1 L/min) and the sampling chamber (22 L/min), and 5% water content in the stack gas, the corresponding Cr aerosol concentration is approximately 57 μg/dscm. For the Cr signal intensity in Figure 4(a) (points 1 - 75) and the 3-σ standard deviation for the blank (points 300 - 400), the signal is a factor of approximately 13 times higher than the detection limit. This corresponds to a Cr aerosol LOD of approxi-

mately 4.4 μg/dscm. The Cr signal intensities measured during the RM-29 sampling were actually slightly higher than that measured for the first 75 points in Figure 4(a). The average signal intensity measured for these prior time scan data files, acquired during the RM-29 sampling, corresponds to a uniform Cr solution concentration of 6.3 ppm, or 63 μg/dscm Cr during the RM-29 run. Based on the standard deviation of the signal levels detected during the RM-29 sampling and later, for the Cr calibration spiking data, the determined concentrations may not be statistically different.

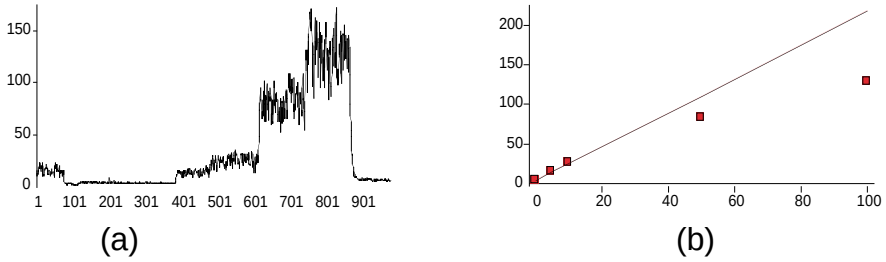

FIGURE 4. (a) Time scan monitoring data for chromium (Cr (I) 359.35 nm), with metals introduced into the stack, water introduced into the stack, and Cr calibration spikes added to the sampled gas stream. (b) Calibration curve for Cr, generated from the time scan data.

For Be and Pb, similar calibration spiking experiments were performed. The time scan data and corresponding calibration curves for Be and Pb are shown in Figure 5. For beryllium (Be (II) 313.11 nm), the signal intensity variations were severe, using a 1-s integration time, approximately 60% rsd. However, by averaging the signal intensities over approximately 100 points for each region in Figure 5(a), a reasonable calibration curve (Figure 5(b)) can be generated, despite the large variations in time scan data. A larger signal variation for the Be time scan data was observed during the testing (Figure 5(a)), compared to that observed for Cr (Figure 4(a)). The larger rsd for Be signals compared to those for Cr and Pb is presumably due to the Be line being an ion line, while the Cr and Pb lines are atom lines, and that the sample flow variations into the air-ICP affected ion lines

more significantly than atom lines, at least for the plasma operating conditions used during the testing. Using the Be calibration curve, the measured Be intensity is equivalent to a solution concentration of 5.2 ppm Be, for the stack metals signal in Figure 5(a), points 1 - 190. The corresponding aerosol concentration is approximately 52 μg/dscm Be. This concentration is close to the detection limit for Be, for the experimental conditions during the testing. The signal to noise ratio for the Be time scan data (points 1 - 190 for the Be signal and points 200 - 300 for the blank standard deviation in Figure 5(a)) is less than two.

For the calibration spiking experiments for lead (Pb (I) 405.78 nm), an integration time of 3-s per point was used, which lowers the signal variation of the time scan data in Figure 5(c) to about 20% rsd. For the calibration curve in Figure 5(d), the 100-ppm Pb spike solution data was not included in the linear regression fit of the time scan data. The error in the fit of the calibration curve was improved significantly by excluding this point. The reason for the lower signal intensity (19% lower than the fitted intensity) for the 100-ppm Pb spike solution is unknown. It is not a detector saturation problem, such as that for Cr in Figure 4, but apparently due to instability from an unknown source. A solution concentration equivalent to 4.4 ppm Pb is calculated for the stack metals signal in Figure 5(c), points 1 - 50, using the Pb calibration curve. The corresponding Pb aerosol concentration is approximately 44 μg/dscm. The signal to noise ratio of the Pb time scan data in Figure 5(c) is a factor of approximately 3, calculated for the Pb signal intensity (points 1 - 50) and the 3-s standard deviation of the water blank (points 60 - 100 in Figure 5(c)). Therefore, the detection limit for Pb is approximately 15 μg/dscm for the conditions used during the test run. During the RM-29 sampling period, higher signal intensities (than that shown in Figure 5(c), points 1 - 50) were measured for Pb in the sampled stack gas. The average intensity for these prior time scan data files corresponds to a solution concentration of 5.6 ppm Pb, or approximately 56 μg/dscm for Pb, during the RM-29 sampling. For Pb, different CCD detector

integration times were used for the calibration spiking experiment (Figure 5(c)) and the prior time scan data files acquired during the RM-29 run. The 56-µg/dscm value for Pb was calculated assuming that the signal intensities for Pb and for the blank scale linearly with detector integration time.

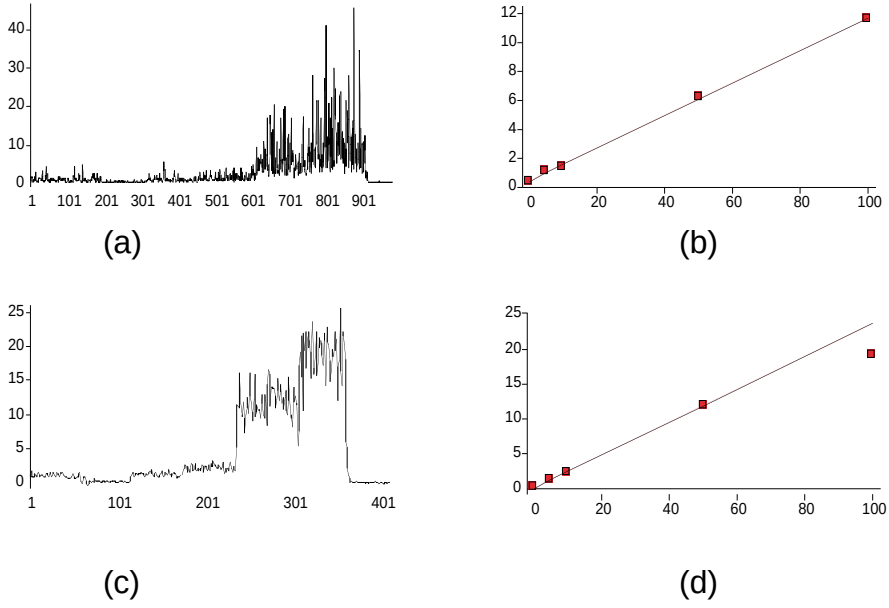

FIGURE 5. Time scan calibration spiking data for (a) beryllium (Be (II) 313.11 nm) and (c) lead (Pb (I) 405.78 nm), with metals introduced into the stack, water introduced into the stack, and calibration spikes added to the sampled gas stream. Calibration curves for (b) Be and (d) Pb, generated from the time scan data.

During acquisition of the second RM-29 sample set on September 16, metals were introduced into the stack at levels identical to those used during the first run. The air-ICP signal intensities for Be, Cr, and Pb during the RM-29 sampling were approximately equal to those measured earlier in the day. Time scan monitoring for Cr and Be during the second RM-29 run is shown in Figure 6. These time scan data files were acquired using a detector integration time of 3-s per point,

so the rsd of the signal variation is less than that shown above for Cr in Figure 4(a) and Be in Figure 5(a). For Cr in Figure 6(a), the rsd is 12.3%. In Figure 6(b), the rsd for the Be signal is 35% and 47% for points 1 - 39 and points 60 - 178, respectively. For the approximate 1-minute time period between points 39 and 60, the Be signal dropped significantly. This decrease resulted from a large increase in the sample gas flow into the air-ICP system, while momentary adjustments in the operating conditions of the stack were made. These normal variations in stack operations were made throughout the testing period, with resulting obvious changes noted in the time scan data collected using the air-ICP and in the differential pressure indicated by the oil filled manometer on the inlet to the axial channel of the plasma. Fortunately, after these momentary changes in stack operating conditions occurred, the signal levels detected using the air-ICP system returned to values observed prior to the stack fluctuation. A second example of this is shown in time scan data in Figure 4, during the initial time that the blank was introduced into the stack, approximately points 80 - 125 in Figure 4(a). After the RM-29 sampling was complete, calibration spiking experiments similar to those shown in Figures 4 and 5 were unfortunately not done for Be, Cr, and Pb. Actually, this calibration spiking should have been done throughout the entire day, before, during, and after the RM-29 sampling. If these experiments had been done during the entire testing period, more useful and meaningful data would have been collected. These results would have provided information on whether the different signal intensities measured during the RM-29 sampling were due to variations in the operating conditions for the air-ICP plasma and sampling system, or whether the signal differences were due to variations in the stack. Approximate metal concentrations in the stack throughout the RM-29 run could have been calculated from these calibration spiking experiments, but some assumptions regarding the signal levels for the blank would have to have been made.

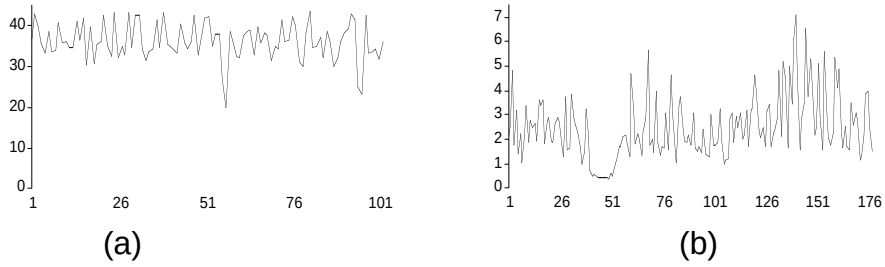

FIGURE 6. Time scan monitoring for (a) chromium (Cr (I) 359.35 nm) and (b) beryllium (Be (II) 313.11 nm) during the second RM-29 sampling conducted on September 16. The detector integration time used was 3-s per point.

Conclusions

The first field test of a continuous sampling air-ICP system was performed at the Diagnostic Instrumentation and Analysis Laboratory (DIAL) at Mississippi State University in September 1999. The system consists of an air plasma that is operated inside a metal enclosure at a pressure slightly less than atmospheric pressure to draw sample continuously into the air-ICP. A Teflon sampling chamber has been designed to allow continuous isokinetic sampling of an exhaust stack or process line for introduction into the plasma, from which optical emission from the metals in the sampled gas stream can be continuously monitored using a spectrometer system such as the AOTF-echelle spectrometer. Concentrations of Be, Cd, Cr, Hg, and Pb were added to the stream of exhaust gases from the fuel oil air furnace on the combustion test stand, and Be, Cr, and Pb were measured with the continuous sampling air-ICP CEM at the ~50 μg/dscm level during the test.

All of goals of the test were accomplished, although with varying degrees of success. First, we had planned to integrate the reduced pressure plasma system with the matching network and solid state RF power supply at DIAL. This task was successfully accomplished. Second, we planned to integrate the AOTF-echelle spectrometer at

DIAL, with the reduced pressure air-ICP system. This was accomplished. However, due to the failure of the AOTF, we were forced to modify the spectrometer for the duration of the test, by using a small grating spectrometer instead of the AOTF as a predisperser for the echelle spectrometer. This substitution allowed the test to go forward, although time limitations and problems associated with aligning the modified spectrometer ultimately led to poorer detection limits for Be, Cd, and Hg during the test, compared to previous laboratory values. The detection limits determined during the test should not be considered indicative of the capabilities of either the AOTF-echelle technology or the reduced pressure air-ICP. Third, we planned to assemble the CEM system and attach it to the test stand facility at DIAL. This goal was successfully accomplished. Fourth and finally, we planned to use the CEM to monitor metals in the exhaust line. This goal was accomplished. The CEM was used to monitor for three of the five target metals while DIAL staff simultaneously collected RM-29 samples for later analysis. These analyses are not yet complete, but when they are, we will amend this report with those results and comparisons with our data. The performance of the CEM in this stage was limited by the problems with the modified spectrometer and by an unanticipated problem with pressure fluctuations in the exhaust stream. The spectrometer and alignment issues were unavoidable at the time and will be corrected in future field tests. The pressure fluctuation issue will be corrected with some fairly minor modifications to the sampling system. Overall, the test was extremely successful in that we accomplished all of the ambitious goals that we set out for ourselves, and we learned some valuable lessons that will be used to improve the system in future tests and demonstrations.

Future Work

One of the most significant issues that was experienced during the field testing at DIAL was the substantial amount of sample flow variation to the plasma, as a result of the pressure fluctuations in the exhaust line of the combustion test stand. During future testing at

DIAL, this situation will be compensated for by installing a sample flow ballast between the sampling chamber and the sampling pump. The ballast will provide a nearly constant pressure reservoir for secondary sampling into the plasma, thereby providing a nearly constant sample flow to the air-ICP. The ballast will be installed between the pump and the secondary sampling region in the Teflon chamber, so that the isokinetic sampling will not be affected. A ballast volume of about 33 L would result in a flow time constant of 99 s, for a sampling rate of 20 L/min. This time constant corresponds to a maximum pressure variation of about 1% per second. Another possible improvement involves increasing the velocity of the sample gas in the heated transfer line and decreasing the conductance of this line. Reducing the diameter of the transfer line will increase the velocity and reduce the conductance of the flow of sampled gas from the exhaust pipe to the sampling chamber. This change will decrease the magnitude of the pressure variations in the sampling chamber. It should also have the effect of decreasing the transit time of the sampled gas from the exhaust pipe to the ICP torch, presumably resulting in greater sample integrity and reduced particle fall out.

One question that was not addressed during this first test was the impact the present of particulate material will have on the operation of the continuous sampling system. This potential problem will be addressed in the test planned for next year at DIAL.

References and Related Publications

1. David P. Baldwin, Daniel S. Zamzow, David E. Eckels, Robin Wiser, Shiquan Tao, and George P. Miller. September 1999. Testing of a Continuous Sampling Air-ICP System as a Continuous Emission Monitor at the Diagnostic Instrumentation and Analysis Laboratory. Ames Laboratory-US DOE Report IS-5138.

- D.P. Baldwin, D.S. Zamzow, D.E. Eckels, and G.P. Miller 1999. AOTF-Echelle Spectrometer for Air-ICP-AES Continuous Emission Monitoring of Heavy Metals and Actinides. In *Environmental Monitoring and Reme-*

diation Technologies, T. Vo-Dinh and R. L. Spellicy, eds. Proceedings of SPIE Vol. 3534, pp. 478-486.

- D.P. Baldwin, D.S. Zamzow, D.E. Eckels, and G.P. Miller. September 1999. A Continuous Sampling Air-ICP for Metals Emission Monitoring. Submitted for publication in the Proceedings of the International Conference on Environmental Monitoring and Remediation Technologies II, Proceedings of SPIE Vol. 3853.

- G.P. Miller, Z.Zhu, D.P. Baldwin, and D.S. Zamzow. 1997. DOE/EPA. Test Results from the DOE/EPA Sponsored Multi-metals Continuous Emission Monitor Demonstration: A Portable ICP-AES System for On-line Monitoring of Toxic Metals. Final Report.

Detection of Toxic Compounds by Cavity Ring-Down Spectroscopy

Ram Vasudev

Introduction

The goal of this project is to apply cavity ring-down spectroscopy (CRDS) to the detection of toxic compounds, the current emphasis being on chlorinated organic compounds of environmental concern. For a general description of the technique and experimental setup, the reader is referred to our earlier reports.

Recent Work

Work is continuing on acquiring spectra of chlorinated aromatics by CRDS and on improving the detection limits. We are finding that the absorption wavelengths are quite sensitive to the location of chlorine substituents on the phenyl ring (i.e., the molecular structure). In addition, the band shapes (rotational contours) are also sensitive to

molecular structure. These spectroscopic properties will be useful for distinguishing different toxic compounds (including structural isomers) in eventual field experiments. Work is also continuing on spectroscopic simulation programs for comparison of experimental results with calculations. These results will be the subject of a paper to be submitted for publication.

Future Plans

Work will continue on toxic compounds of interest to DOE and those in EPA's TRI list.

Volatile Organic Compound Monitoring Using Diode Lasers

C. P. Winstead

Introduction

The United States Department of Energy currently operates three mixed waste thermal treatment facilities (TSCA at Oak Ridge, WERF at INEL, and CIF at Savannah River). A clearly identified need for these facilities is continuous emission monitoring for a number of volatile organic compounds (VOCs). For example, Table II of the Savannah River Site Technology Need Statement #SR-1004 lists 16 organic species as potential candidates for continuous emission monitoring at the CIF. The primary motivations for application of CEM technology at the CIF are reducing or eliminating the need for periodic trial burn testing and reducing the scope of required feed testing. Increased public confidence in incinerator operations is also an important by-product of CEM implementation. A savings of approximately $108M is estimated to result from successful installation of

CEM technology at the CIF alone. In addition, numerous other DOE sites and facilities are interested in trace VOC measurements (e.g., widespread interest in measurements for TCE).

Diode lasers are extremely small and relatively inexpensive compared to other laser and spectroscopic systems. Because of similarities in vibrational frequencies for carbon hydrogen bonds, absorption of diode laser light will be observable for a variety of VOCs over a wavelength range of approximately 1.6 - 1.8 micrometers, a region accessible to quantum well distributed feedback diode lasers. Such lasers exhibit long lifetimes and robust performance and are well developed for telecommunications applications. Thus, quantification of diode laser detection limits for VOCs is desirable for applications in continuous emission monitoring or other environmental measurement applications. The concentration of VOCs in air can be determined by measuring the amount of laser light absorbed as the beam crosses a known pathlength of air.

Our initial measurements are focusing on long pathlength diode laser absorption spectroscopy. Should lower detection limits be required, these initial results will pave the way for future increased sensitivity methods such as diode laser cavity ringdown spectroscopy. An eventual organic CEM product is envisioned where multiple lasers are multiplexed into a single fiber for introduction into a sample cell. By modulating each laser at a different frequency or at different times, multiple species measurements can be carried out using a single fiber optic cable and one detector. Demodulation of the signals can yield multiple species measurements with one fiber much the same way multiple telephone calls are carried on one fiber.

The experimental configuration used for these initial investigations is depicted in Figure 7. Precision current and temperature controllers are used to drive the output from the diode laser. The wavelength of the laser is roughly controlled by laser temperature while fine wavelength control is exerted using the laser current. The

output beam from the diode is directed into a multipass cell which, depending upon the number of passes that the beam makes through the cell, can be set for an optical pathlength of up to 50.4 meters. A mechanical vacuum pump is used to evacuate the cell and various gases are subsequently added when absorption measurements are to be made. The pressure in the cell is measured using a capacitance type pressure gauge. The laser light exiting the cell is detected on a photodiode detector connected to a lock in amplifier. The ratio of light transmitted by the cell both with and without a sample gas present is used to calculate the total concentration of sample present. A beam splitter placed between the laser and the cell can be used to divert a fraction of the laser beam, providing a reference signal unperturbed by absorption in the cell. A frequency generator can be employed to modulate the diode laser current and provide a reference signal for the lock in amplifier. The actions of the laser controller and the data acquisition are all managed by a personal computer.

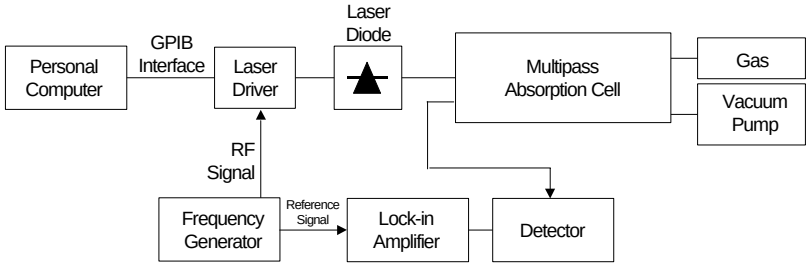

FIGURE 7. Experimental configuration for diode laser absorption spectrometry

Work Accomplished

The system depicted in Figure 7 was employed to make near atmospheric pressure measurements of trace levels of benzene in nitrogen and air. To accomplish these measurements, it was necessary to upgrade the sample introduction system to allow better control over the quantity of benzene introduced into the cell. To produce part

per million levels of benzene at atmospheric pressure in the sample cell would require an initial introduction of a very low pressure of benzene prior to introducing the air or nitrogen. Measuring such low pressures in the cell using a pressure gauge would be very inaccurate. Instead, a volume ratio system was constructed whereby a higher pressure of benzene was introduced into a much smaller cell. The benzene from this cell is then allowed to expand into the larger volume of the sample cell. By repeating this process initially with high pressures of nitrogen, the volume ratio of the sample cell to the small cell can be determined. The high pressure measured in the small cell is divided by the volume ratio to calculate the pressure of benzene introduced into the sample cell.

Figures 8 and 9 depict the results of benzene absorption experiments carried out using 1656 nm light in 730 Torr of nitrogen and air, respectively. This pressure is just slightly below atmospheric pressure so that the sample will not leak from the vacuum cell. This slight reduction has no significant effect on the results, as is evidenced by comparison of Figures 8 and 9 with previously reported low pressure data. The change from vacuum to higher pressure experiments actually slightly increases the sensitivity of the measurements for benzene. While this may seem counter to usual experience, the basis for this result is that the benzene spectrum is already very broad even at low pressures due to overlapping rotational transitions. Hence, the broadening of individual rotational lines does not cause a reduction in sensitivity. The slight increase in sensitivity could be due to changes in the relaxation time of the excited vibrational level caused by gas collisions. Although the wavelength of the laser used for these studies was not optimized for benzene detection (the laser was constructed for monitoring CH_4), an atmospheric pressure detection limit of 140 ppm for benzene in air was achieved. By obtaining a diode laser operating at a wavelength near the peak of the benzene absorption, this detection limit can be improved by a factor of six - seven times, implying a benzene detection limit of approximately 20 ppm for the 47.6-meter pathlength sample cell configuration used here. Focusing

on electronic noise reduction could no doubt lower this detection limit by up to an order of magnitude.

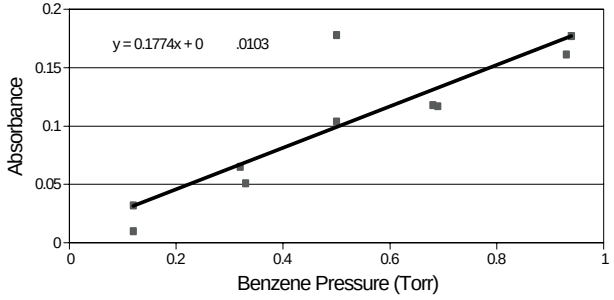

FIGURE 8. Absorbance measurements for benzene in 730 Torr of nitrogen with diode laser temperature set at 35°C.

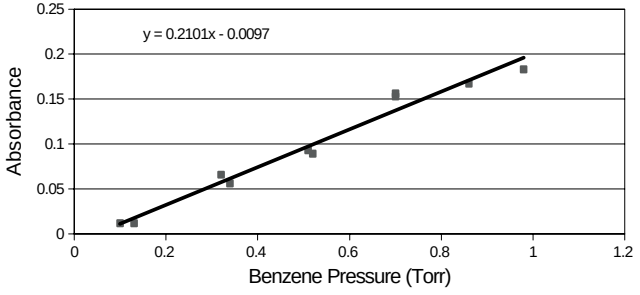

FIGURE 9. Absorbance measurements for benzene in 730 Torr of air with diode laser temperature set at 35°C.

Work Planned

For the next quarter, we plan to investigate the response of the system for small concentrations of chlorobenzene under vacuum conditions and in nitrogen and air at atmospheric pressure. This is important to evaluate the response of the system at the same wavelength for a different species. A common problem in introducing benzene into

vacuum systems is that adsorption onto the cell walls causes the pressure of benzene to drop rapidly, introducing some scatter into the observed data. Examining the response for chlorobenzene should help in determining how large a factor this effect has on our benzene data.

Nomenclature

VOC	volatile organic compound
CEM	continuous emission monitor
FM	frequency modulation

Laser Induced Fluorescence Spectrometry of Radionuclides

David L. Monts

Introduction

Purpose

The purpose of the Laser Induced Fluorescence (LIF) project is to provide the U.S. Department of Energy (DOE) with a robust, cost effective technique capable of rapidly and accurately determining the concentrations and isotopic abundances of long lived radionuclides (such as uranium and plutonium) without the need for lengthy sample preparation. Knowledge of isotopic abundances is necessary since different isotopes can have widely differing activities. The niche for this technique is determination of concentrations and isotopic abundances for cases where current techniques are severely limited by low

throughput such as: (1) cases where the radioactivity is so low that radioactive decay disintegration counting techniques cannot analyze samples during acceptable counting periods; and (2) cases where lengthy sample preparation is required for mass spectrometric determination. For these situations, LIF can save tax dollars by reducing or eliminating holding batch samples for time consuming analyses. In addition, since this technique is applicable to a wide variety of other species, it may also be deployed as a monitor of other species of concern, such as Tc.

Methodology

Laser induced fluorescence (LIF) spectrometry is a well established, robust technique for detecting species of interest at low concentrations. In the LIF technique (Fig. 10), an electronic state of the species of interest is excited with a tunable laser and the resulting fluorescence intensity is monitored as a function of laser wavelength. Since the mass of isotopes are different from one another, the corresponding atomic energy levels are slightly different (Fig. 11). Consequently, when a sufficiently high resolution tunable laser is scanned across an atomic electronic transition, the resulting LIF spectrum contains a peak associated with each isotope present; the intensities of the isotopic peaks are directly related to the concentration of the isotope. Hence, the isotopic abundances can readily be obtained from the LIF spectrum. In order that the individual isotopic transitions can be resolved, it is necessary that the species of interest be in the gas phase. For the TRU elements of interest, an atomization source is required in order to volatilize and atomize the sample. A calibration curve is obtained by recording the LIF signal intensity as a function of concentration. Using the calibration curve, unknown concentrations can be determined.

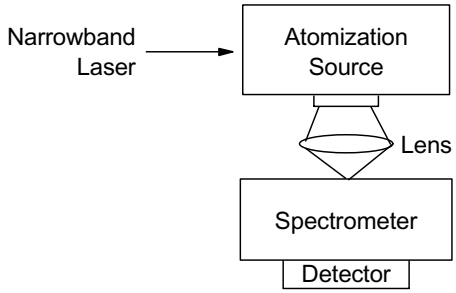

FIGURE 10. Schematic of the laser induced fluorescence spectrometry technique.

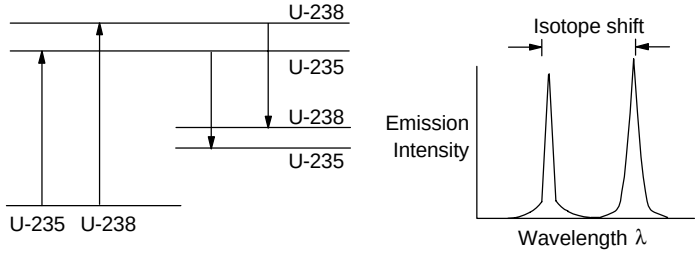

FIGURE 11. Schematic of isotopic energy shifts and the associated LIF spectrum.

Work Accomplished

In order to make progress on the use of LIF for isotopic determination of TRU elements, there are three prerequisite needs that must be meet. The first is the capability to work with actinides, such as uranium. Mississippi State University's license has been extended to permit controlled usage of elements with atomic numbers in the range of 84 (Po) through 98 (Cf). The license extension was granted to the university, and the university had the required capabilities to begin implementing the license in July. An application to the university's Radiological Safety Committee for permission for us to perform the laser induced fluorescence spectrometry experiments on dilute ura-

nium solutions was approved during August, contingent upon us having in place a dedicated vent line and standard capabilities for routinely working with radiological samples. Construction of the dedicated vent line began and was almost completed; delay in delivery of HEPA filters for the vent line precluded completion during this quarter.

The second prerequisite need is the need for a sufficiently hot atomization source in order to efficiently atomize uranium. During January, an ICP atomization source was ordered with a promised delivery date in May. This ICP atomization source was not delivered during May; in fact it was not delivered during either the second or third quarter of 1999. Because of the prolonged delay in delivery of this essential piece of equipment, progress on this project was severely hampered during this quarter since the next group of experiments require this equipment. Therefore during this quarter we concentrated most of our efforts on our other projects for DOE.

Work Planned

When the ICP atomization source is received, we will begin a series of experiments to optimize operation of the ICP system initially using argon as the carrier gas and surrogates and then uranium as the analyte species.

The third prerequisite need for successful completion of this project is for a sufficiently narrow linewidth, tunable laser system that can be reproducibly scanned. DIAL's cavity ringdown spectroscopy group will permit us to use their new moderately high resolution dye laser system to perform some preliminary experiments in an ICP plasma. If, as expected, these LIF experiments prove that such a moderately high resolution tunable laser system has sufficient resolution for the TRU elements, then funds for purchase of a comparable dye laser system will be requested for FY 2000; if the experiments indicate that even higher resolution is required, then additional funding

will be sought in order to purchase an ultra high resolution tunable laser system.

Nomenclature

DIAL	Diagnostic Instrumentation and Analysis Laboratory
ICP	inductively coupled plasma
INEEL	Idaho National Engineering and Environmental Laboratory
LIF	laser induced fluorescence
nm	nanometer
ppm	parts per million
TRU	transuranic

Cavity Ringdown Monitors for Transuranic Elements

C. P. Winstead and G. P. Miller

Introduction

The Idaho National Engineering and Environmental Laboratory has expressed a need for monitoring residual transuranic (TRU) elements in treated high level waste. Specifically, a need exists for on-line monitoring of the low activity fraction of this treated waste after dissolution and partitioning. Such a system could replace expensive off-line sampling and analysis and eliminate the need for holding tanks in the Idaho HLW process. However, detecting TRU elements

at ultra sensitive levels has proven to be problematic for traditional radiological counting methods due to the long half lives of these predominantly alpha emitter elements.

Cavity ringdown is a relatively new variant of absorption spectroscopy that has demonstrated extreme sensitivity in a variety of studies. In pulsed cavity ringdown spectroscopy, a pulse from a tunable laser is introduced through the end mirror of a stable optical cavity. This optical cavity is formed from two highly reflective mirrors, and serves to trap the fraction of the laser pulse that enters the cavity. The laser pulse interacts with an absorbing medium in the cavity for up to thousands of cavity round trips. The reflectivity of the mirrors and the absorption of the sample in the cavity determine the decay time for the pulse. As the absorption in the cavity increases, the decay time for the light in the cavity decreases. By inserting into the cavity an appropriate atomization source, such as an inductively coupled plasma or graphite furnace, very low concentrations of the various chemical forms of TRU elements can be atomized and detected using cavity ringdown.

The primary objective of this project is to evaluate cavity ringdown spectroscopy as a technique for detecting and monitoring transuranic elements. No ringdown measurements of uranium or transuranic elements have been carried out to date. If these measurements prove to have the necessary sensitivity for monitoring needs, a monitor based on a ringdown method could be developed for DOE. This work is directly applicable for many DOE sites, including INEEL and Hanford as mentioned above, and if successful will likely find use in all DOE focus areas.

Work Accomplished

Due to regulatory requirements, no cavity ringdown measurements for transuranic elements were carried out during this time period. A new ventilation system has been completed to allow the use

of radioactivity in our experiments. This system was part of the permitting process for allowing our use of such material. All that is required is the completion of the licensing procedure for the use of radioactive elements. In the meantime, we have continued to optimize the operating parameters for both an inductively coupled plasma system and graphite furnace to enable their use as an efficient atomization source and have demonstrated the use of both systems for a number of metallic elements. Thus, we are in position to investigate the performance of cavity ringdown spectrometry for uranium monitoring in both inductively coupled plasma and graphite furnace systems once final approval is given. A publication entitled "Preliminary Results for Electrothermal Atomization - Cavity Ringdown Spectroscopy (ETA-CRDS) was published in *Analytical Communications*, V36 (7), 277 (1999). Also during this time period, an invited book chapter for an upcoming edition of *Encyclopedia of Analytical Chemistry* on laser absorption cavity ringdown spectrometry for analytical chemistry applications was revised and accepted for publication.

Work Planned

Upon receiving the appropriate permits and final approval to use uranium, we will carry out a number of experiments to determine the performance of cavity ringdown for uranium monitoring. Our initial efforts will focus on an evaluation of detection limits for uranium using cavity ringdown spectrometry. These efforts will provide the information necessary to decide whether cavity ringdown has application as an on-line monitor for transuranic elements and uranium. Detection limits and the ability to discriminate isotopes will be evaluated.

Feasibility of Characterizing Solid Wastes by Remotely Sensed Multispectral Images

David L. Monts

Introduction

Purpose

Characterization capabilities for site specific wastes are needed for the DOE nuclear waste cleanup program. Many wastes are heterogeneous and have a mixture of both RCRA hazardous constituents and radioactive species in various forms and matrices. Characterization requirements vary from waste stream to waste stream. For example, some wastes have high radiation fields and therefore require characterization to be completed at some distance from the actual waste containers. Some wastes may require nonintrusive characterization. Currently however, comprehensive nondestructive testing (NDT), assaying (NDA) and examination (NDE) techniques do not exist for effective waste characterization. In the field of remote sensing, airborne imaging spectrometers have been used to mineral identification. For example, the vibrational overtone features for Al-OH (2.16 to 2.22 μm) has been used to identify minerals containing kaolinite [$Al_2(Si_2O_5)(OH)_4$]. The value of the technique lies in its ability to acquire a high resolution reflectance spectrum for each pixel in the image. Vibrational absorptions from compounds of heavier elements occur in the mid infrared region. Not only will a portable remotely sensed imaging spectrometer system will provide nonintrusive, nondestructive characterization of solid wastes, it also will overcome some of the obstacles of the existing technologies (sample collecting, preparation, costly and timing consuming analysis). It is well established that the infrared spectrum can be used as a “fingerprint” to identify and characterize molecules. The species of concern (RCRA and radioactive elements) will be present primarily as com-

pounds. Irradiation with an infrared light source will permit collection of reflectance spectral images.

Methodology

Compounds can be characterized by the spectrum of light that they absorb. In particular, the infrared spectral region contains a number of (vibrational) transitions that can be utilized to thoroughly characterize compounds. Absorption spectra can be obtained either by recording the light transmitted through a sample or by recording the light reflected off a sample. Transmission of light for generating absorption spectra is not an economically feasible option for the waste streams of interest to DOE. Therefore, as shown in Figure 12, the method under study consists of recording infrared light reflected off a sample. Instead of using a spectrometer to record the spectrum of the reflected light, a multispectral imaging system (MSIS) will be used in the final configuration. For the feasibility study experiments performed here, an infrared spectrometer and infrared detector will be utilized. Both scanning infrared spectrometer and a Fourier transform infrared (FTIR) spectrometer will be used in these efforts.

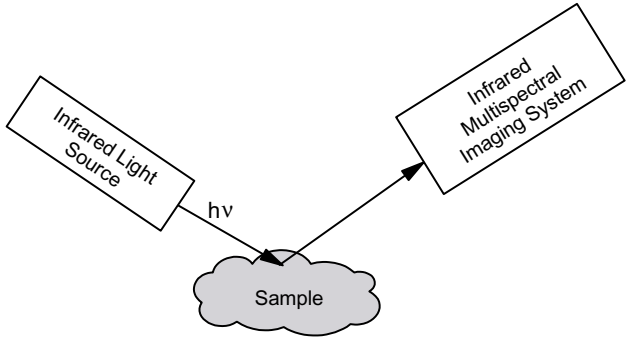

FIGURE 12. Schematic of infrared diffuse reflectance multispectral imaging technique (final configuration).

Work Accomplished

During this period, we found that the available infrared light sources did not have sufficient intensity for the proposed experiments and have utilized available funding to place an order for a high intensity infrared light source with an anticipated delivery of four to six weeks after receipt of order.

Work Planned

When the high intensity infrared light source is received, we will initiate a series of experiments using several known, pure compounds that can be expected to be present in the waste streams.

Nomenclature

DOE	U. S. Department of Energy
FTIR	Fourier transform infrared
MSIS	multispectral imaging system
NDA	nondestructive assaying
NDE	nondestructive examination
NDT	nondestructive testing
RCRA	Resource Conservation and Recovery Act

Guided Wave Nondestructive Evaluation Technique Development and Demonstration

Krishnan Balasubramaniam

Introduction

Corrosion and cracks in metal components constituting the pressure boundary poses a significant safety concern at nuclear storage and handling facilities of the Department of Energy - Environment Management (DOE-EM) facilities.

Project Significance

The Tri Party Agreement (TPA) schedule requires retrieval of wastes in the Single Shell Tanks (SST) to begin by 2004 for future vitrification and permanent storage in a waste repository. There is already an ongoing effort in the structural integrity assessment of the Double Shell Tanks (DST). A rapid nondestructive evaluation of tank wall and liner integrity needs to be performed prior to the selection of a retrieval method to assure successful retrieval of the waste from the tank. For example, in the case of a hot cell liner, if it can be determined that the cell liner is intact, an aqueous decontamination method can be used. Otherwise, a dry method must be deployed at a significantly greater cost. In the case of SSTs, sluicing is considered to be one of the primary methods to retrieve waste. It is possible that sluicing may not be a viable method for retrieval of tanks which have extensive corrosion damage. Other more expensive techniques may have to be employed for damaged SSTs. A rapid integrity assessment program for the tanks is needed in order to (a) estimate life time of the tanks and liners and prioritize the tanks with shortest remainder life for retrieval, and (b) evaluate new techniques for retrieval of damaged tanks which may have leaked.

Background

Cracks (both through wall and non through wall cracks) and corrosion damage on tank walls and hot cell liners is a high priority concern. These flaws must be evaluated to determine the potential for tank rupture and estimate rates of leaks that may occur in the future and assess appropriate actions. Visual inspection is not the answer since most of the damage may not be visible due to buildup on the walls. Also, it is difficult to quantify the extent of damage, especially in the thickness direction, using visual techniques.

The current method uses a point by point ultrasonic or eddy current NDE approach to this evaluation and employs advanced signal processing methods to characterize damage. This is a rather cumbersome and time consuming method. Also, damage detection is currently considered feasible, but damage quantification has not been reliable. The approach proposed here using guided waves can be used to rapidly ascertain the existence of cracks or corrosion larger than the critical size. Often this critical size is greater than 75% of wall thickness and in most cases a through wall damage identification is sufficient. Here, the ultrasonic waves are generated at one end of the structure and detected at the other end and a 180-degree sweep will cover the entire tank wall. These tanks are large and many of them are buried with access only to riser penetrations in tank domes, which are 12 inches in diameter. To overcome this access problem, we proposed to design this sensor, during the implementation phase, onto a robotic manipulator arm mounted on a telescoping mast such as the Light Duty Utility Arm System (LDUA) developed by Westinghouse Hanford Company for the visual inspection of such tanks.

Damage of the metallic components is suspected due to the long period of operation and the corrosive media which is being stored and handled. The low confidence in the currently available Nondestructive Evaluation (NDE) techniques to accurately determine damage could lead to the spread of contamination and/or regulatory concerns

when retrieving the tanks. The corrosion challenges the integrity of the affected structure and may compromise the leak tightness property of the structure. Novel, reliable, remote, and cost effective techniques are needed for the evaluation of the structural integrity of these structures before handling. Successful development and demonstration of this technology will provide a needed assessment tool for assuring safe operation of the nuclear waste handling facilities. Unlike previous work, the proposed work uses remote ultrasonic transaction and has the advantage of long range, multi mode generation/detection, and hence improved safety, sensitivity and reliability of inspection for flaws in nuclear waste storage and handling components.

Methodology

Ultrasonic guided waves can be generated in geometrically narrow structures, such as plates, shells, pipes, and rods due to the effect of the interference of reflected and refracted waves which reverberate between the boundaries of the structure. Based on the geometry of the structures, these wave modes are called plate waves, cylindrical waves, rod waves, etc. These waves are generated and measured using several mechanisms. The exact generation mechanism will depend upon the geometry of the structure. Remote methods of generation can be accomplished using either laser based ultrasonics or using Electro-Magnetic Acoustic Transducers (EMATS). These waves travel long distances, depending on the frequency and mode characteristics of the wave, and follow the contour of the structure in which they are propagating. These wave modes can also be classified, for example, into symmetric, anti-symmetric, and axi-symmetric modes based on the type of cross sectional displacement profile exhibited by the wave during propagation. The use of guided wave modes is potentially a very attractive solution to the problem of inspecting the embedded portions of metal components because they can be excited at one point on the structure, propagated over considerable distances, and received either at a remote point on the structure

in a through transmission mode or back at the point of generation, in a pulse-echo reflection mode. The received signal contains information about the integrity of the metal between the transmitting and receiving transducers.

Although these wave modes propagate longer distances, the presence of waste material limits this range. This is caused by the leakage of energy into the waste. This leaked ultrasonic energy is relatively small and poses no threat to waste material chemistry. The sensitivity of the sensing system will also deteriorate as the range of inspection is increased above a certain distance. Also, there is a mode conversion phenomena when the wave encounters a sharp bend. Hence, in order to evaluate the structure, the sensor parameters such as mode selection, energy generated, transmitter receiver separation, and data interpretation must be optimized.

Most of the work conducted thus far using the guided waves has investigated the inspection of plates, piping and tubing, which are not embedded. It has been demonstrated that nondestructive modes which propagate long distances are sensitive to wall thinning, cracks, and pits that may be present in the material being examined. The long range propagation and detection of the plate wave modes have been optimized and their interaction with defects have been reported. Measurements of 100 meters or more have been demonstrated. Since, each individual mode has a unique cross sectional displacement and stress profile and because several modes can be selectively generated and received using the same set of transducers, it is feasible, even in a field deployable system, to utilize the sensitivities of multiple wave modes and simultaneously measure several damage parameters such as location, size, type, and shape of the damage.

DIAL has the laser ultrasonic capability for remote generation and reception of the ultrasonic guided waves. Wave propagation models are also available at MSU for the simulation and parameter selection in order to conduct efficient experiments. The instrumentation

for conducting experiments with electromagnetic transduction (EMAT) also exists at DIAL.

Work Accomplished

Process Monitoring Sensor. An l8 inch long graphite rods with zirconium coating was design, procured and tested under simulated high temperature conditions at DIAL. Graphite coated with zirconia was tested as the material of choice for the design and fabrication of buffer rod. The coating process was not very reliable due to thermal expansion, contrary to the claims made by the coating process vendor. This lead to the oxidation of the graphite rods. Alumina does not have this problem, but when dealing with long rods, the attenuation in the rod changes with temperature and becomes an issue beyond 1000 C.

Guided Wave Tank NDE Technique. The modeling of the ultrasonic waves using ANSYS code was further developed. The FEM code was further studied to simulate the wave propagation in pipes and the issue of interaction of ultrasonic waves with cracks and interfaces. Also, corrosion damage modeling was investigated. This is a complex problem since there a myriad types of corrosion damage.

Conclusions

The buffer rod material problems remain the key to solving the problem of long distance access to the melt. The technique has been demonstrated using short buffer rods and hence there is confidence in the technology.

Based on the initial results from the guided wave modeling, there is a significant scope for the generation and propagation of guided plate waves in tank walls. Although modeling of corrosion is feasible, it may not be possible to cover all types of corrosion. The effect of

concrete and soil which may be loading the metal tank wall must be investigated.

Project Status

All tasks in the projects are currently active.

Work Planned

Process Monitoring Sensor. It is planned to investigate other types of coatings and buffer rod materials which can withstand high temperatures.

Guided Wave Tank NDE Technique. The modeling of defects in solids will continue. Incorporation of external loading in the form of soil and concrete will be completed by the next quarter.

TASK 2 *Measurement Support*

Measurement services will be provided for DOE sites. In some cases, a specific site will not be able to justify the cost of a new instrument but will need it to achieve a programmatic objective. DIAL can take its instrumentation to the DOE site to provide the measurements needed.

Diagnostic Field Applications Coordination and Testing Support

Robert L. Cook

Activities in this task have been rescheduled to a later date due to man power demands in other tasks.

On-line Imaging for Thermal Treatment Processes

David L. Monts

Activities in this task have been rescheduled to a later date due to man power demands in other tasks.

TASK 3 *Performance Evaluation*

The performance of environmental technologies will be evaluated for DOE. DOE EM needs a tool which will rapidly, and without bias, allow it to compare the performance of technologies against the field's needs, so that it can focus its development dollars on the highest impact targets. DOE EM also needs a tool to rapidly screen new technologies to assist in the most effective allocation of its development funding. Further, the technology developers (and DOE EM) need a tool to expedite the acceptance of developed technologies into the DOE EM user facilities. DIAL is ideally suited to address both of these needs. Through its network of contacts within the DOE sites, DIAL can rapidly elicit user needs. Through its knowledge of the technologies needed, and its network of contacts in industry, DIAL can rapidly identify promising candidates to satisfy those needs. DIAL's experienced multidisciplinary staff can then provide users with the information they need to make deployment decisions, by using DIAL's wide-ranging measurement capabilities in either its own testing facilities, or in those of its network of collaborators if more appropriate for a given application.

Dissolution of Hanford Salt

J. S. Lindner and R. K. Toghiani

Introduction

Project Significance

The Office of River Protection (ORP, formally the Tank Waste Remediation System) is responsible for pretreating the legacy wastes contained in the double and single shell tanks at Hanford and for delivering these streams to the privatization contractor, British Nuclear Fuels Limited. The stored wastes contain three discernible constituents, high ionic strength liquid, sludge and saltcake. Most of the experimental and theoretical modeling efforts to date have been concerned with the sludge and liquid fractions; however, a large portion of the waste, estimated to be 60% by mass in some tanks, exists as saltcake. Recognizing this deficiency, the Tank Focus Area (TFA) issued Technical Response 671:PBSTW05. The efforts described here are the results of a successful proposal funded by TFA with cost sharing from DIAL.

Thermodynamic modeling of complex, multi-component electrolyte solutions at high ionic strengths and with proper consideration of solids formation is a formidable task. Personnel evaluating the waste at Hanford have selected, based on initial comparisons between experimental results and an assessment of available software, the Environmental Simulation Program (ESP, OLI Inc.). The code has subsequently been used for modeling laboratory sludge leaching experiments and tank contents.[2-4] To our knowledge, the work reported here is the first application of the model to saltcakes. The short time period in which ESP has been in use at Hanford suggests, however, that evaluation of the code for different applications is an

evolving process. Thus, the work performed here is implicitly centered on model validation.

All of the work connected with this subtask has been aimed at providing end users at Hanford with additional information regarding the performance of the ESP code. A main goal of the work is to increase confidence in the predictive capability of the model. A proven, validated process engineering tool could result in considerable cost savings. For example, proper modeling of the pretreated waste will indicate the propensity of the waste to foul transfer lines, thereby eliminating the high costs of effecting repairs and slipped delivery schedules. In addition, analytical characterization of the large volume of waste at the site (55 million gallons), along with the process streams that will be generated upon retrieval of the waste, is impractical. A tool is needed which can describe the waste and associated process streams with sufficient reliability such that costly characterization studies can be minimized.

Background

The previous work at Hanford has indicated some limitations in the application of ESP.[2-4] Solid-liquid equilibrium (SLE) model calculations have been found to agree with laboratory results for aqueous solutions containing most of the pertinent single salts (NaCl, $Na_2C_2O_4$, $NaNO_3$, etc.). At elevated ionic strengths, however, the solubilities from the model are less than experimental observations. Consequently, the code predicts higher solids loadings, and this has potential ramifications on the privatization contract through the amounts and types of diluents used for pretreating the waste.

Other questions regarding the code concern the quality of the data used in the integral software databases. Analytical results on the tank wastes at Hanford have indicated the presence of a number of double salts such as Na-F-PO_4, Na-F-SO_4 and Na-SO_4-CO_3. Literature data on these systems are rare. What results are available indicate that var-

ious types of solids structures, crystals and gels can result depending on composition. Natrophosphate, $Na_7F(PO_4)_2 \cdot 19H_2O$, for example, has been observed to form gels.[5,6] Sodium phosphate, $Na_3PO_4 \cdot XH_2O$, can form different crystal structures depending on the extent of hydration. Accurate modeling of the partitioning of the solids and liquid phase constituents will only be as good as the fundamental data used in the model.

Methodology

Some identified options for validating the ESP code include:

- comparisons to experimental data on actual tank samples;
- determination of the SLE behavior for those systems which are of direct importance to the end users at Hanford and where literature results are fragmentary;
- comparison of the results of the model to other thermodynamic models; and
- examination of the thermodynamic data called by the code.

Little is known about the pretreatment requirements of saltcakes, and experimental studies on this portion of the waste are lacking. An evaluation of the predictive capabilities of the ESP model is possible by comparing code predictions with the results of experimental studies. Other comparisons of the model to tank sample analysis include direct customer requests.

Critical evaluation of the fundamental thermodynamic constants called by the model permit an assessment of the quality of the data used by OLI Inc. and can identify possible error sources. In many instances, especially with regard to the double salts systems cited above, sufficient data does not exist in the literature and any compilation will only consider the available information as estimates. Determination of the solubilities and associated phase diagrams for

selected systems provides a means for ensuring the quality of the experimental data and a path for model sensitivity calculation.

Different theoretical representations can be used to calculate the SLE behavior of aqueous systems. Comparison of the results from ESP with other thermodynamic models allows an independent check on the thermodynamic framework used and may also indicate deficiencies in the ESP model or associated database.

Work Accomplished

Data are presented and discussed regarding the comparison of ESP with the actual saltcake dissolution experiments that have been performed at Numatec Hanford Corporation (NHC).[7,8] These experiments have provided insight into the proper use of the ESP software and also on information or database limitations that currently exist. Additional calculations on issues relating to electroneutrality reconciliation are presented to fortify the calculation presented in the previous quarterly report.[9] The contribution forms a portion of a paper that will be submitted to the Waste Management Conference to be held in Tucson in February of 2000.

Data preprocessing and charge reconciliation. Experimental measurements to determine the total composition of the saltcake composite samples retrieved from four tanks were performed by Herting.[7,8] The analytical data consisted of the weight percent of the various cations and anions in the composite as well as a weight percent of water contained in the sample. The data were converted to concentrations (using an estimated density) and then input to the Water Analyzer (WA) program within ESP (version 6.0). The WA component is a front end processor for laboratory analytical data and performs charge reconciliation and adjusts the water content in the mixture such that experimental cation and anion loadings are achieved in the output molecular stream. The input concentration data may exhibit a slight charge imbalance due to analytical uncertainties.

Data were subjected to charge reconciliation, and the molecular streams generated within the WA module were used in subsequent ESP process simulations. Table 3 provides a summary of species present in the four tanks examined in this work.

TABLE 3. Major constituents in saltcakes (weight percent of sample).[a]

	TANK			
	BY-102	BY-106	A-101	S-102
H_2O	16.7	14.7	31.2	~5
Al^{+3}	1.65	1.59	2.39	.67
Cr^{+3}	.2	.11	.17	
Fe^{+3}	.05	.02	.014	
K^{+}	.09	.24	.31	.07
Na^{+}	27.77	25.06	21.20	22.99
TIC*	4.13	1.43	1.81	.59
$C_2O_4^{-2}$	.53	1.26	1.35	.17
Cl^{-1}	.13	.16	.41	.16
F^{-1}	1.17	.62	.07	
NO_2^{-1}	1.85	2.72	7.43	2.04
NO_3^{-1}	10.92	40.68	12.6	53.72
OH^{-1}	1.09	1.14	2.1	.42
PO_4^{-3}	.6	.34	.38	.52
SO_4^{-2}	5.12	1.17	2.44	.32

[a]Data from references 7 and 8

*Total inorganic carbon (CO_3^{-2}/5)

The charge imbalance present in the analytical data can be rectified in the WA module through the addition of a dominant ion or by the user selecting a specific ion or through a proration process. In the

later calculation, the makeup charge is equally distributed over all of the anions or cations.

The reconciliation method was determined to have a significant impact on subsequent process simulations. Typically, the charge imbalance found in the initial data was on the order of 1 to 8% and all four tanks examined, prior to reconciliation, had a net negative charge. Use of the dominant ion reconciliation method resulted in the addition of sodium to balance the charge. Since the majority of solid species that will undergo dissolution as diluent (water) is added to a saltcake sample are sodium salts, the addition of sodium can adversely impact ESP predictions of saltcake dissolution through overestimation of the amount of the various salts present in the solid phase.

The makeup ion or user choice method allows the adjustment of an individual cation or anion to achieve neutrality. Depending on the magnitude of the net charge in the input data, the amount of selected ion is increased or decreased. Again, the addition or subtraction of a single species to adjust the charge can result in an overestimation or underestimation of salts containing this species in the solid phase.

Proration adds an equal percentage of each cation to the sample composition if a net negative charge is computed from the analytic data (or of each anion, if a net positive charge is computed). This method allows the net charge imbalance to be distributed among the various cations (or anions) present.

The impact of selecting a specific mode of charge reconciliation on the adjusted cation and anion concentrations for tank BY-106 is provided in Table 4. As anticipated, the use of the dominant ion or the makeup ion methods leads to a significant change in one ion concentration compared to the others. The proration method, however, leads to electro-neutrality with the impact more uniformly spread over either all cation concentrations or all anion concentrations. For this

example, all cation concentrations were increased to balance the original negative charge of the laboratory data. Consideration of the impact of this adjustment on the generated molecular stream and examination of the subsequent saltcake dissolution experiment simulation output (see below) confirmed that the proration method of charge reconciliation provided a more uniform mechanism for adjusting the net charge imbalance.

TABLE 4. Impact of charge reconciliation method on adjusted ion concentrations - Tank BY-106.

Species	Original Input (mg/L)	Dominant Ion (Na^-) (mg/L)	Makeup Ion (NO_3^-) (mg/L)	Proration (mg/L)
Al^{3+}	24682	24226	26003	25889
Cr^{3+}	1760	1727.5	1854.2	1846.1
Fe^{3+}	298	292.49	313.95	312.58
K^+	3776	3706.2	3978.1	3960.7
Na^+	3.8847e+05	4.1133e+05	4.0926e+05	4.0747e+05
OH^-	82209	80689	86608	80812
Cl^-	2536	2489.1	2671.7	2492.9
CO_3^{2-}	1.1111e+05	1.0906e+05	1.1706e+05	1.0922e+05
F^-	9580	9402.9	9580	9417.2
NO_2^-	42166	41387	42166	41450
NO_3^-	6.3051e+05	6.1886e+05	5.773e+05	6.1980e+05
$C_2O_4^{2-}$	19569	19207	19569	19237
PO_4^{3-}	5301	5203	5301	5210.9
SO_4^{2-}	18105	17770	18105	17797

Ideally, one could reconcile the charge imbalance using both cation and anion concentrations. For example, tank BY-106 exhibits a net negative charge of approximately 6.7%. An increase of the overall cation equivalence by 3.35%, along with a decrease of the total anion equivalence by 3.35%, would result in a net zero charge. This method

of charge reconciliation is not available in the current release of ESPs but can be accomplished manually and was evaluated. Anion concentrations from the subsequent dissolution experiment simulation were not significantly impacted; however, the availability of proration within the WA module appears to be equally effective and was employed for the saltcake dissolution simulations.

Table 5 provides a summary of the molecular streams generated by WA for tank BY-106 using the different charge reconciliation methods. The differences in the composition of the streams are quite noticeable; yet, these compositions provide equilibrated streams for the ESP process module that have the appropriate loading of the various cations and anions and approximately the same percent water. The primary reason for the large differences in molalities for the molecular species between the dominant ion/proration methods and those for the makeup ion method is the significant reduction in nitrate concentration for the makeup ion method.

TABLE 5. Impact of charge reconciliation method on generated molecular stream - Tank BY-106.

Species	Dominant Ion (Na^-) (molality)	Makeup Ion (NO_3^-) (molality)	Proration (molality)
H_2O	55.509	55.509	55.509
$Al(OH)_3$	228.056	32.6802	242.527
$Cr(OH)_3$	8.43866	1.20924	8.97419
$Fe(OH)_3$	1.33026	.190628	1.41472
H_2CO_3	438.116	62.7815	436.625
H_6F_6	19.7921	2.8363	19.7259
HCl	17.8326	2.55541	17.7730
HNO_2	228.497	32.7427	227.732
HNO_3	2535.08	315.720	2526.59
KOH	24.0767	3.4502	25.605
$Na_6(SO_4)_2CO_3$	23.4910	3.36651	23.4126

TABLE 5. Impact of charge reconciliation method on generated molecular stream - Tank BY-106.

$Na_7F(PO_4)_2.19H_2O$	6.95755	.997002	6.93426
NaOH	4354.76	576.474	4290.87
$H_2C_2O_4$	55.4249	7.94238	55.2417

In addition to supplying the experimental ionic concentrations, the user must enter a density. Adjustment of the density allows tuning of the generated molecular stream to reproduce the experimentally measured percent water in the sample. This iterative procedure insures that the stream developed in WA and routed to the process module is representative of the loading of cations and anions in the analyzed sample. The process also reduces the impact of the estimated density used to initially convert the original analytic data in weight percent to concentrations (in mg/L) for input to the ESP WA program.

In all studies presented in this paper, the proration method has been used for charge reconciliation, and the input density was adjusted to achieve the experimentally measured percent water in the original saltcake sample. This is the same process that was proposed to Hanford for automation of the WA module.[9] Experimental percent water measurements and the predicted percent water from ESP are summarized in Table 6. A detailed listing of the molecular streams generated for each tank by the WA program is not included here, but is available.[10]

The composite sample for Tank S-102 was extremely dry, and the percent water was determined experimentally to be 5%. However, Herting[11] indicated that the percent water was more likely to be closer to 11% based on mass balance calculations. The low water content prevented tuning of the input density in WA to allow the experimental percent water to be achieved; convergence problems arose as the input density was reduced in an attempt to achieve the 5% by weight water value. The lowest predicted percent water which could be

achieved in the generated molecular stream for S-102 was ~16% by weight. This much higher percent water impacted the predictions for the saltcake dissolution experiments for tank S-102. Examination of the water loadings in the three other tanks investigated indicated absolute errors of less than 0.6%.

TABLE 6. Comparison of predicted percent water with experimental measurements.

Tank	Experimental Weight % H_2O (Herting[7,8])	ESP Prediction of Weight % H_2O
BY-102	26.53	26.4
BY-106	14.75	14.9
S-102	5	16.2
A-101	31.2	31.8

Saltcake dissolution experiments. The dissolution experiments were conducted at 25˚C and 50˚C.[7,8] Detailed experimental procedures are provided in the references, and only a summary of the procedure is given here. Known amounts of saltcake from a given tank core sample and diluent water were combined and mixed thoroughly to promote dissolution. The samples were then allowed to equilibrate and centrifuged, and the liquid was decanted. The weights of the solid constituents and supernate were obtained. The liquid samples were then analyzed for specific gravity, weight percent water, and select anion concentrations (chloride, fluoride, hydroxide nitrate, nitrite, oxalate, phosphate, sulfate, TIC and TOC). The liquid samples were diluted during the analytical procedure; consequently, all species were fully ionized (i.e., aqueous $NaNO_3$, present at higher ionic strengths, was converted to Na^+ and NO_3^-). The percent dilution by weight ranged from 50% to 300% (100% dilution by weight was defined as 100 g of saltcake mixed with 100 g of diluent). For the 50˚C experiments, the saltcake and diluent were mixed, and the solution was heated and allowed to equilibrate. The samples were then centrifuged and analyzed as described above.

Simulation of saltcake dissolution experiments. The ESP process model for this experiment consisted of three unit operations, a MIX block, a HEATER block, and a SEPARATE block. In the MIX block, the molecular stream describing the overall saltcake composition for a particular tank (generated within the WA module) was combined with the appropriate amount of water and mixing was accomplished at 25˚C and 1 atm. The outlet stream from the MIX block flowed into the HEATER block where the temperature was adjusted to the laboratory equilibration point (25˚C or 50˚C). The effluent from the HEATER block was then routed to a SEPARATE block where the stream was partitioned into the relevant (solid and liquid) phases.

The unit operations for the process simulation required the development of a Chemistry Model that described the relationships controlling the intra phase and inter phase equilibria between the ionic, aqueous and solid species present. The number of equations needed to account for the various species is directly related to the number of species defined in the WA (data preprocessing) module. ESP has limitations on the number of aqueous and solid species that can be described, and exceeding these limits results in an error. The model must then be refined to exclude molecules and ions that are not expected to form. In the case of the wastes at Hanford, and the ionic strengths and pH values encountered in this work, those species that nominally contain one or more hydrogen atoms (aside for input stream composition requirements) can be omitted. In all simulations described here, the models automatically generated by ESP were, however, used with only a single modification. Dawsonite, $NaAlCO_3(OH)_2$, was excluded as a possible solid species on the basis of discussions with Hanford personnel.[12] In addition to the Public database available within ESP, two private databases denoted $NaNO_3$ and Trona were used. The $NaNO_3$ database contained the correct sodium nitrate data from an earlier release of ESP (version 5.4); predictions of $NaNO_3$ chemistry in version 6.0 were found to be substantially different than that observed in version 5.4 and OLI Inc. supplied a patch database to correct the problem.[13] The Trona database was

invoked following the realization that the Public database did not properly describe the behavior of sodium carbonate hydrate(s) at high ionic strengths (see below).

Saltcake dissolution was simulated over the range of 0% to 500% by weight addition of water, thereby encompassing the experimental measurements. Comparison of the simulation predictions with the experimental data required a significant amount of post processing. In the ESP prediction of the aqueous stream, nitrate ion will be found in various forms including the dominant species NO_3^- and $NaNO_{3(aq)}$. The contributions of each constituent containing nitrate ion in the liquid phase were summed after appropriate weighting. For example, the contribution of nitrate from $NaNO_{3(aq)}$ was found by multiplying the weight of $NaNO_{3(aq)}$ by the ratio of the molecular weight of nitrate ion to that of sodium nitrate. Calculations for other nitrate containing components were performed and then the total nitrate concentration was obtained from the sum of all of the nitrate fractions over the volume of the aqueous stream. This provides a prediction for the nitrate concentration that is functionally equivalent to that obtained from the decanted liquid in the actual experiments. The predictions for the other anion components were determined in the same way.

Comparison of ESP predictions with the experimental results of Herting[7,8]. The data in Figure 13 compares the predicted (ESP) and experimental nitrate concentrations for all four tanks as a function of percent dilution by weight. Solid sodium nitrate was initially present in all saltcake compositions. As water was added, the solid underwent dissolution resulting in an increase in the nitrate anion concentration. Once all of the solid sodium nitrate has dissolved, the total amount of nitrate anion in the supernate liquid will remain constant. As water was added, the concentration decreased reflecting increased dilution.

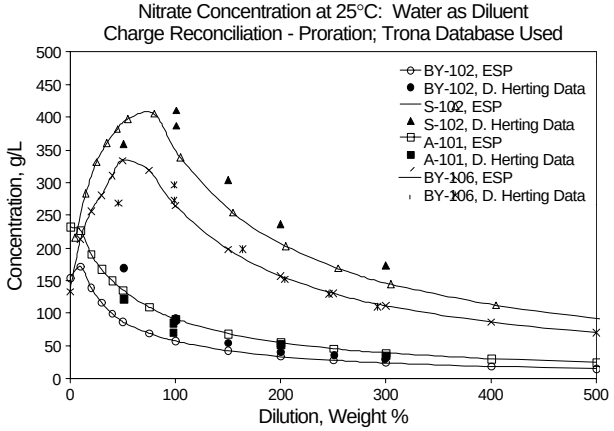

FIGURE 13. Comparison of the ESP predictions of nitrate concentration with experimental data of Herting.[7,8]

The agreement between the experimental measurements and predictions is quantitative at higher dilution levels (> 100%). For both tanks BY-106 and S-102, the weight percent of nitrate in the undiluted saltcake (Table 3) was much higher (40.68% and 53.7%) than for tanks A-101 (12.6%) and BY-102 (10.92%). These differences are reflected in the much higher concentrations realized for nitrate in the liquid supernate. For tanks BY-102, BY-106 and A-101, the model predictions of nitrate concentration are within the experimental error of the measurements at the dilution levels > 100%.

Differences between prediction and experiment were found for the S-102 saltcake even at high dilution levels. It is important to note that the maximum concentration of nitrate predicted by ESP is 405 g/L and that at 100% dilution by weight the experimental measurements of nitrate concentration were 387 g/L and 410 g/L. The agreement in the maximum concentrations confirms that the generated molecular stream used as input to ESP contains the appropriate loading of nitrate. If the generated molecular stream had significantly higher nitrate loading, the predicted maximum concentration of

nitrate would also be elevated. The trend evident in the experimental nitrate concentration data is reflected in the ESP predictions; however, there is a systematic shift of the predicted concentrations relative to the experimental concentrations. The experimental concentrations were found to be slightly higher than the predicted concentrations at any given level of dilution (for percent dilution by weight $\geq$ 100%). Since the generated molecular stream contained larger percent water by weight than the experimental data (16% versus 5%), the difference in concentrations could, in fact, be accounted for by the failure of the program to allow convergence at the lower water loading. A rough estimate of the predicted concentration that might be realized if it were possible to achieve the 5% water is 338 g/L/(.89) = 382 g/L at 100% dilution. This compares more favorably to the reported experimental concentrations of 387 g/L and 410 g/L at this level of dilution.

In the low dilution region (< 100% dilution by weight), only a single experimental measurement at 50% dilution by weight was available. Here, considerable amounts of solids were predicted to remain in the saltcake sample. The largest fraction of these solids arose from the sodium salts, and in addition to sodium nitrate, sodium carbonate monohydrate and sodium oxalate were predicted to be present along with the double sodium salts, natrophosphate, $Na_7F(PO_4)_2 \cdot 19H_2O$, and sodium-fluoride-sulfate, $NaFSO_4$.

The dissolution behavior of the double salts has been found to significantly impact the dissolution of the single salts that are present. The predictions for phosphate, fluoride and sulfate for those tanks where fluoride was present (all but S-102) all deviate from experimental data. Figure 14 provides a comparison of predicted sulfate concentrations and the experimental data.[7,8] Tank BY-102 contained the largest weight percent of both sulfate and fluoride of the four tanks examined (ratio of F^-/SO_4^{2-} ~ .228, total weight percent of these two components ~ 6.3%). Thus, the sodium fluoride sulfate double salt is predicted to be present in the solid phase until dilutions of

greater than 100%. The general behavior of the dissolving double salt in BY-102 is mirrored by the predicted concentrations. For tank BY-106, which also contains moderate amounts of sulfate and fluoride (ratio of F^-/SO_4^{2-} ~ .53, total weight percent of these two components ~ 1.8% by weight), this same behavior is reflected for the sulfate concentrations. However, for tank A-101, which contains only a small amount of fluoride (ratio of F^-/SO_4^{2-} ~ .028, total weight percent of these two components ~ 2.5%), only a small amount of the sodium fluoride sulfate double salt is predicted to be present in the solid phase (2.3% by weight of the solid phase). The prediction of sulfate concentration by ESP is in agreement with the trend displayed by the experimental data for tank A-101. For tank S-102, for which the composite saltcake sample contained no fluoride (at detectable levels during total composition by sequential dissolution tests), the agreement between ESP predictions of the sulfate concentration and the experimental sulfate concentration data is within experimental error for the sulfate concentration. Similar behavior is exhibited by the phosphate concentrations predicted by ESP as well. ESP predicts that the phosphate in the tanks containing fluoride is found in the solid phase as the sodium-phosphate-fluoride double salt.

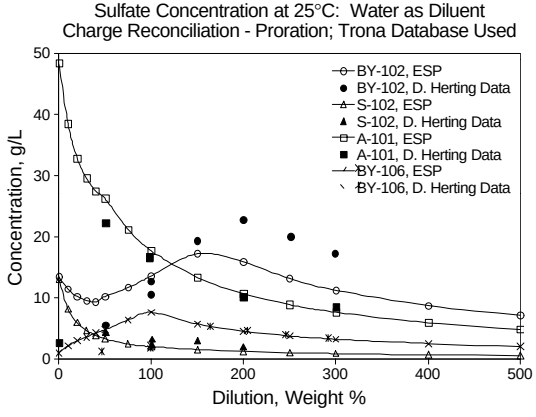

FIGURE 14. Comparison of ESP predictions of sulfate concentration with experimental data of Herting.[7,8]

It is hypothesized that these discrepancies arise from inadequacies in the thermodynamic data contained within the ESP Public database, i.e. the source database for the double salt thermodynamic data. Errors in the fundamental data for the sodium double salts will also impact the predicted equilibrium behavior of the single sodium salts such as sodium nitrate and sodium carbonate monohydrate. For tank S-102, the absence of fluoride in the saltcake, compared to the other three tanks where fluoride was present, resulted in improved predictions of all anion concentrations in the low dilution region (< 100%). When fluoride is present in the saltcake, ESP predicts that the phosphate and sulfate in the solid phase are found in the double salts, $Na_7F(PO_4)_2{\cdot}19H_2O$ and $NaFSO_4$. It was initially unclear whether the deviations in predicted phosphate and sulfate concentrations were due to ESP incorrectly predicting the solid phase species or due to the quality of thermodynamic data for the double salts in the ESP Public database.

As part of an effort to confirm ESP predictions of the presence of double salts in the dissolving saltcake, Herting carried out crystal identification on the species present in the solid phase for BY-102 saltcake.[8] Sodium carbonate monohydrate, sodium nitrate, sodium fluoride-sulfate, natrophosphate and sodium oxalate were all identified in the solid phase using polarized light microscopy and other techniques.[8] The solid phase predicted by ESP also contained all of these species. This confirms that ESP is properly predicting the species present in the solid phase. Any discrepancies between experiment and prediction are therefore due to the quality of thermodynamic data for these double salt systems. Laboratory efforts are underway to measure the solid-liquid equilibria for these double salts as a function of temperature and ionic strength.[14] These measurements can then be used to improve the quality of the thermodynamic data included in the ESP database.

Figure 15 compares the predicted concentrations for TIC (total inorganic carbon) with the experimental data.[7,8] Inclusion of the

Trona database to provide thermodynamic data for $Na_2CO_3 \cdot 1H_2O$ was necessary to correctly predict the behavior of carbonate under the high ionic strength conditions realized in these Hanford tanks. Use of the ESP Public database incorrectly predicted that sodium carbonate monohydrate would initially not be present. In fact the Public database did not predict that this molecule would be present in the solid phase resulting from dilution levels less than 100%. For tank BY-102, which contained significantly more TIC than the other tanks examined, experimental characterization of the solid phase indicated the presence of the monohydrate of sodium carbonate.[8] In order to predict its existence in the solid phase, the Trona database had to be employed. The relevant thermodynamic data for this monohydrate that allows the prediction of the solid phase forming at lower temperatures due to the higher ionic strength present in the system. As evidenced in Figure 15, the solid phase for BY-102 is predicted to be predominantly composed of this monohydrate of sodium carbonate. At a dilution level of ~ 50% by weight, the monohydrate is predicted to be completely dissolved and further addition of water results in behavior typical of dilution. Predictions of TIC concentration in the low dilution region (< 100%) do show some discrepancy with experimental measurements except for the prediction of TIC in tank S-102. An examination of the hydrate transition temperature as a function of ionic strength for the sodium carbonate system being initiated will attempt to provide an improved understanding of this behavior under conditions relevant to the Hanford tanks.[14] Data obtained through this effort can then be used to improve the predictive capability of ESP.

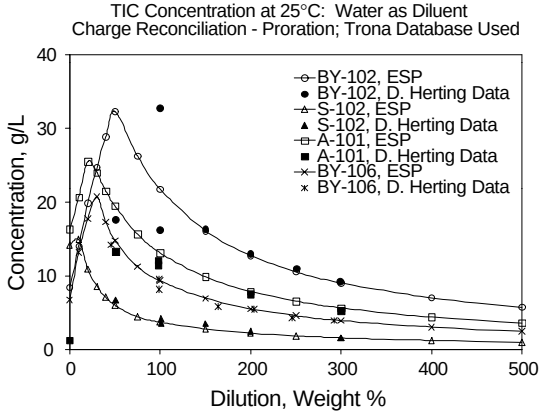

FIGURE 15. Comparison of ESP predictions of TIC concentration with experimental data of Herting.[7,8]

Conclusions

Evaluation of the application of ESP as a modeling tool for predicting the dissolution behavior of saltcakes present in the Hanford tank is in progress. An iterative approach to balance charge for the experimental analytic data supplied to Water Analyzer has been developed which allows the generated molecular stream used in subsequent ESP calculations to properly reflect the cation and anion loadings as well as the percent water in the experimental data. Saltcake dissolution has been modeled using ESP. General trends exhibited by the experimental data are also exhibited by the ESP predictions. These predictions and their comparison to experimental data also indicate a need for improved thermodynamic data for the sodium double salts present in the waste and a need for improved understanding of the relationship between hydrate transition temperature and ionic strength.

Project Status

Solid-liquid equilibrium experiments for the double salt Na-F-PO_4 system as a function of temperature and ionic strength are in progress. Efforts are also in progress to compare theoretical predictions between ESP and Solgasmix for this system. Additional experiments and simulations wherein supernate fractions are combined are needed. These later efforts will provide insight into the possible formation of solids under certain retrieval conditions.

References

2. G.T. MacLean. 1994. Computer Simulation of Laboratory Leaching and Washing of Tank Waste Sludges. WHC-SD-WM-E%-312. Westinghouse Hanford Corporation, Richland, WA.

3. D.A. Reynolds. 1995. Practical Modeling of Aluminum Species in High pH Waste. WHC-EP-0872.Westinghouse Hanford Company, Richland, WA.

4. R.K. Toghiani, J.S. Lindner, C. Barfield and E.C. Beahm. October 1999. Saltcake Dissolution Modeling, FY 1998 Status Report. DIAL 40395 TR 98-1.2. Diagnostic Instrumentation and Analysis Laboratory, Mississippi State University.

5. C.F. Weber. May 1998. A Solubility Model for Aqueous Solutions Containing Sodium, Fluoride and Phosphate. Ph.D. Dissertation. The University of Tennessee, Knoxville.

6. E.C. Beahm, et al. 1998. Status Report on Solid Control in Leachates. ORNL/TM-13660. Oak Ridge National Laboratory, Oak Ridge, TN.

7. D.L. Herting and D.W. Edmondson. 1998. Saltcake Dissolution FY 1998 Status Report. HNF-3437, Rev. 0. Numatec Hanford Corporation, Richland, WA.

8. D.L. Herting, D.W. Edmondson, J.R. Smith, T.A. Hill and C.H. Delegard. 1999. Saltcake Dissolution FY 1998 Status Report. HNF-5193, Rev. 0. Numatec Hanford Corporation, Richland, WA.

9. J.S. Lindner and R. K. Toghiani. Last Quarterly Report.

10. R.K. Toghiani and J.S. Lindner. January 2000. Saltcake Dissolution Modeling, FY 1999 Status Report. DIAL 40395 TR98-1.4. Diagnostic Instrumentation and Analysis Laboratory, Mississippi State University.

11. D. Herting. 1999. Personal communication.

12. G. MacLean. 1999. Personal communication.

13. J.S. Lindner and R.K. Toghiani. April 1999. Thermodynamic Simulation of Tank 241-SY-101 Dissolution- Part 3 Crust Solids Dissolution Modeling and Associated gas Release. DIAL Letter Report DIAL 40395 TR 98-1.3. Diagnostic Instrumentation and Analysis Laboratory, Mississippi State University.

14. J.S. Lindner and R.K. Toghiani. Work in progress.

Wall Removal Monitor

Gary Boudreaux

Introduction

One technique for the decontamination and decommissioning (D&D) of concrete structures within the Department of Energy and the nuclear industry is to remove a layer of material from the surface using a technique known as scabbling. The agency responsible for D&D of the facility, the contracting agency, generally specifies to the scabbling contractor the depth of material to be removed, e.g., 0.5 inch off the surface of a floor or wall. Under current practice, measurements are made, before and after, at discrete points on the wall

with laser based survey instruments. Feedback is on the order of days, instead of hours or minutes. With near real time feedback the contractor can remove the correct amount of material the first time avoiding both repeating a costly visit and generating more waste than is warranted. Another obvious limitation to this technique is that there is no way to be sure that the contractor has met the specification between survey points, which can be a foot apart.

Another method to deal with the problem is to weigh the amount of concrete that is removed. The average depth of material removal can then be calculated by measuring the density of a small sample cut from the surface. The feedback from this technique is almost immediate, but it does not take into account variations in depth of removal or density that can occur in practice. Thus, a technique that can measure the amount of material removed over a given area and in near real time would benefit both the agency and the contractor. A wall removal monitor has been developed at DIAL to serve this need. The monitor uses Fourier transform profilometry (FTP), which is an imaging technique that can measure the surface profile of an object.

The FTP technology, based on image processing techniques implemented at DIAL, can measure the profile of a surface. When a pattern of straight lines is projected onto a surface, the pattern is distorted or warped by irregularities. Areas of the object that are closer to the camera cause the lines to squeeze together and areas farther from the camera cause the lines to spread apart. This difference in line spacing provides information on the shape, or profile, of the surface. If changes are being made to the surface then images of the surface need to be acquired, both before and after the change, from the same position. When the two images are compared, then changes in height can be determined. It is particularly well suited, but not limited to, relatively flat surfaces.

The system consists of a standard slide projector, a digital camera (a video recorder or film camera can also be used), and a computer.

The projector and the digital camera are mounted on a tripod, which can be placed anywhere from two to 30 feet from the surface in question. However, this distance affects the size of the area being imaged; a larger area can be imaged by setting up farther away from the surface. A grid of lines is projected onto the surface and an image is captured with a digital camera. The image is processed on the computer in order to determine the profile information.

The wall removal monitor can be operated in harsh environments, is easily calibrated in the field in a matter of seconds, and can currently run in near real time. Advances are being made to allow the process to run in real time. The spatial resolution (the distance between points on the surface) depends on the area of the surface being imaged. If a one square foot area is imaged, the spatial resolution turns out to be approximately 0.01 inches. For comparison, the spatial resolution of the laser based techniques is on the order of several inches or feet. The resolution in the depth direction depends on several factors: the spacing and contrast of the grid lines; the size of the area being imaged; and the background "noise" in the image. Taking these considerations into account, 0.1 inch is a reasonable estimate of the depth resolution for the concrete scabbling application.

Work Accomplished

We have kept good contact with the Waterways Experiment Station and provided them with a copy of the trip report and explained the results. They now have the technology and have made some measurements on their concrete structures/targets. We have begun the process of applying for a copyright on the code that has been completed so far.

A Phase I SBIR was considered (with Miltec) to use the WRM to measure solar cell vibration on satellites.

Conclusions

A system has been demonstrated in a real world scenario that can accurately measure large areas with a high degree of precision on "noisy" surfaces. The system has been constructed with the durability of fieldwork in mind and uses easily attainable commercial parts. All necessary calibration field measurements are quick and easy to make, and processing is in near real time. FTP fits the role of wall removal monitor well, as it can measure a surface profile relative to the original surface. From the depth information gathered using FTP, it is possible to calculate volume of material removed, point wise depth removal, and minimum and maximum depths of removal. Although a surveying method is capable of such calculations, the data is so sparse that numbers for point wise measurements are useless. Finally, the system can be used at the job site while the contractor is working, potentially saving the contractor and the contracting agency time and money by preventing costly revisits, ensuring quality, and providing accurate measurement archival.

Work Planned

We will continue to seek a commercial partner to commercialize the technology for this and other applications. We plan to convert the software to LabWindows/CVI windows C-base platform. We will find and test a better light source such as a xenon strobe light. We will also try to improve the density of the phase shifter slide. We will continue to expand the capabilities of the system to handle other applications.

Related Publication

- M.E. Henderson and R.D. Costley. Wall Removal Monitor. DIAL Technical Memo, WRM 1198.

Pipe Decontamination

Gary Boudreaux

Introduction

The Department of Energy has radioactive and hazardous contamination inside many of its process piping and duct systems. Contaminants remain in these systems after liquid is drained from them, adsorbing onto metal and other surfaces or depositing as residual liquids or solids. Many of the piping systems are not directly accessible because parts of them are buried underground or under concrete floors. A tube cleaning system (TCS) has been developed at Mississippi State University (MSU) in collaboration with the Tennessee Valley Authority (TVA) and the Southwest Research Institute (SwRI). The TCS utilizes repetitive high voltage electrical discharges in water or other fluids to produce acoustic shock waves which are effective in removing scale, silt and other fluid saturated deposits from tube inner surfaces. The TCS minimizes the generation of secondary waste while at the same time minimizing worker exposure to radiation.

The TCS uses repetitive high voltage electrical discharges in fluids (principally water) to produce acoustic shock waves. Laboratory and field testing has shown these shock waves to be very effective in removing scale, silt, and other fluid saturated deposits from the interior walls of steam condenser and heat exchanger tubes. This method is a noncontact, nonchemical method for removing these deposits. The necessary equipment, developed under this program, includes a high voltage power modulator (i.e., power supply) to generate the high voltage, high current electrical pulses, and an applicator tip that can withstand the intense stresses caused by the acoustical and electrical pulses.

The arc discharge applicator tip is mounted on a coaxial cable which can be in excess of one hundred feet long. As the cable enters the pipe, it passes through a water tight bushing to prevent the egress of contaminated water. As the applicator assembly is fed into the container, the remotely located power modulator transmits electrical pulses via a long coaxial cable to the applicator assembly which produces acoustic shock waves that are directed at the interior pipe wall. The pulsed acoustic shock wave successively removes accumulated scale and other deposits as the arc discharge source is moved down the tube by the TCS operator. Foreign matter scrubbed from the wall by the shock impulse and cavitation is ejected from the wall into the water. Microscopic particles remain in suspension, where they may be removed from the water via conventional means. Field testing of the existing tube cleaning system suggests that the applicator can be fed into the pipe at rates between 0.3 and 1 ft/sec; however, the feed rate may vary considerably with application.

Work Accomplished

The ground fault interrupt (GFI) of the second tube cleaning system, to be built at DIAL, has been designed and tested. The High Voltage Lab has installed the IGBT electronic modules in the original power modulator cabinet. Initial testing was performed by generating sparks in a five gallon bucket.

We have had several conversations with National Heat Exchange Company, and they are delaying the joint demonstration to the beginning of 2000.

We have continued to follow up and answer questions to several companies, GTS Duratek, Schlumberger, Commerce Services Corporation, Allegheny Power and Light, MTSI, and Gap-Tech, which have potential applications for the TCS. We have identified each of their needs and are planning experiments and designs to solve them.

Conclusions

The TCS has been successfully demonstrated at Sequoyah Nuclear Power Plant (TVA) and the Wabash River Coal Fired Plant (Public Service of Indiana) to clean scale and other deposits from 1-in. diameter heat exchanger tubing. This previously developed and demonstrated technology provides an excellent basis for further developing a system that will decontaminate radiologically contaminated surfaces. This method appears suitable for cleaning and decontaminating tubes, pipes, and other cylindrical storage containers capable of containing fluids.

There are several advantages of this technique over existing technologies. The primary advantage is that the exposure of workers to hazardous and radioactive materials is minimized. This is because the cable can be fed through a bushing into the pipe so that workers do not come into contact with the material within the pipe. Further, the generation of secondary waste is minimized, or avoided. The water in the pipes transports the scale out of the pipes. This same water can be reused to clean other pipes after the foreign matter has been separated from it using conventional means (filtration, centrifuge, settling). Since deposits are knocked off the surface of the pipe through its interaction with the acoustic wave, the use of brushes or chemicals is avoided, further reducing the generation of secondary wastes.

Work Planned

The improved Pulsed Acoustic Pipe Cleaner is soon to be completed at DIAL. The cabinet should be completed soon, and the IGBT modules will be fitted and installed. The solid state switch will undergo further testing in actual pipes. We will also design an applicator tip that propels the acoustic pulse forward and may unclog pipes in support of a need of National Heat Exchange and GTS Duratek. Pipes with different types of fouling will be cleaned with this system in order to determine the effectiveness of the TCS for different appli-

cations and to establish operating parameters. We will continue to seek a commercial partner and will schedule an on site demonstration at a DOE facility when the initial testing of the new pipe cleaner is completed.

Related Publications

- R.D. Costley, M.S. Mazzola and M.G. Grothaus. December 1997. Pulsed Acoustical Technique for Decontamination of Piping and Containment Systems. Presented at X-Change'97: The Global D&D Marketplace, Miami, FL.

- M.S. Mazzola, M.G. Grothaus, M. Walch, M. and J. Jones-Meehan. July 1995. New Electrical Control Methods to Prevent Power Plant Fouling. Tenth IEEE Pulsed Power Conference, Albuquerque, NM.

Drum Pressure Monitor

Gary Boudreaux

Introduction

At many waste sites, transuranic (TRU), low level, and mixed wastes are stored in 55-gallon drums. Many of these drums contain hazardous, organic wastes as well. Radiolysis or other physical or chemical processes may result in gaseous emissions inside these drums. When this occurs, the pressure within the drum will increase, sometimes to unacceptable levels. In more drastic cases, these emissions may produce flammable or explosive atmospheres (e.g., hydrogen from radiolysis). Currently, regulatory procedures require that each drum be individually opened and inspected for the presence of hazardous organic waste. This situation will be dangerous for workers if any of the conditions described above exist (high pressure or flammable atmosphere). A nonintrusive technique that would detect any

increase in pressure over ambient would alert workers of potential danger and greatly increase safety. Conversely, it would allow the segregation of suspect drums, and more rapid treatment of safe drums.

A simple, nonintrusive technique has been developed that will allow workers to determine whether a drum is pressurized. The natural frequency of the drum lid is determined by tapping the lid, recording the audible signal with a microphone, and converting the time domain signal to a frequency spectrum using a fast Fourier transform. It turns out that the natural frequency of the lid is a function of the pressure within the drum. These results have been confirmed using finite element analysis (FEA). These results are being used to design a simple, hand held instrument that requires no specialized training to operate and works in real time.

Work Accomplished

We continue to further our understanding of how uncontrollable factors affect the measurement of pressure using modal analysis. We have collected more data on the corrosion studies and time change of the response. Also, several drum vendors were located and documented.

Commercialization of the technology with Military Technologies (Miltec) continues. The SBIR proposal was rejected, and steps were taken to assure success of future proposals. Kelly Ausbrooks (Safety Officer at the gaseous diffusion plant in Paducah, KY) was contacted about writing a letter to indicate a need for the technology. Whitney St. Michel from INEL was contacted about an RFP that was published concerning a need for a drum pressure detection device.

Conclusions

It has been demonstrated that the frequency of vibration of the lid on a 55-gallon drum is proportional to the pressure inside the drum. This dependence of frequency on pressure is being used to develop an instrument that will detect pressurization within drums. It was shown, however, that different type drums may require different calibrations, i.e. those with and without stiffening rings.[15]

The ultimate goal of this work is to design an instrument that can test drums for pressure in the field. A prototype has been built. This instrument would ideally be hand held, utilizing a microphone, which has certain advantages over an accelerometer. By using a microphone an inspector would save time, since contact with the drum would be minimized. The inspector would simply tap the drum, the signal would be recorded with a microphone that was either internal to the device or attached to a lapel, the signal would be recorded, and the inspector would move on to the next drum. Another advantage is that the spectrum from the microphone signal is usually much simpler, since many of the higher modes do not radiate acoustically. Thus, the spectrum is easier to interpret with software.

More information can be obtained from the frequency response of the lid. Although the goal is to design a simple instrument capable of quickly and efficiently locating pressurized vessels, it has been determined that the fill level of the drum can be determined from characteristics of the drum response. In addition, the time it takes for the signal to dampen can be used to distinguish between different types of contents.

Work Planned

We will continue building the database for corroded lids. We will also continue building the statistical database looking for similarities

and differences between drum lids by manufacture and lot. We will continue to seek a commercial partner and plan to resubmit an SBIR type proposal.

Reference

15. H. Patel, R.D. Costley, M. Henderson, E.W. Jones, and A. Tomlinson. 1999. Drum Pressure Monitor. To be published in *Review of Progress in Quantitative Nondestructive Evaluation*, Vol. 18. D.O. Thompson and D.E. Chimenti, eds. New York: Plenum Press.

Plasma Treatment of VOCs and Other Off-gas Components by Pulsed Micro Hollow Cathode Plasma Array

George P. Miller

Introduction

Low pressure hollow cathode devices are used for a number of applications, most commonly as a narrow line width source lamp. The possibility of operating these devices in air at atmospheric pressure opens up a wide range of opportunities including the destruction and removal of VOCs from exhaust off-gas streams.

Operation in air is achieved by reducing the cathode opening to approximately 100 microns in diameter.[16] This study reported that, at atmospheric pressure, the electric power for a single discharge was measured at 8 W with a gas temperature in excess of 1000 K.

The device is very simple and consists of two layers of metal separated by an insulator (mica) with a hole approximately 100 microns in diameter punched through the top metal and insulator layers. A

potential difference is applied across the two conductors causing the plasma discharge to form. Due to the low power requirements for each micro hollow cathode, it is simple to connect a number of these devices in parallel to form a plasma array over which the gas to be treated flows.

There are several advantages of this technique. It is simple and inexpensive to develop and can be operated at a high gas temperature. It can also be built to the size required.

Experimental Arrangement and Analysis

A system is envisioned where TCE is introduced into an air stream passed through the plasma. Emission spectroscopy will be used to obtain information on the plasma processes. At low gas temperatures, VOCs can be converted to intermediate products that may require further treatment. For example, removing CCl_4 from air using an e-beam produces phosgene as one of its end products. The end products will be analyzed using diode laser atomic absorption, FTIR and GCMS. The gas will then be bubbled through water to remove HCl and other end products and then trapped with a cold trap or vented out of the building. Subject to the results of this analysis, a plasma chemistry model will be developed to allow the rapid optimization of the technique.

VOC Candidate

While many possible VOC candidates present themselves, one example of interest to DOE, is the remediation of trichlorethylene (C_2HCl_3 or TCE). TCE is a major solvent contaminant for which alternative remediation methods are sought. TCE makes an ideal candidate for plasma remediation since it reacts in the gas phase with atomic oxygen and hydroxyl radicals, components that are efficiently manufactured in low temperature plasmas. In remediating TCE, the ideal stoichiometry is

$$C_2HCl_3 + 4OH \text{ ----> } CO_2 + 3HCl + H_2 \quad \textbf{(EQ 2)}$$

$$C_2HCl_3 + 4O \text{ ----> } 2CO_2 + HCl + Cl_2 \quad \textbf{(EQ 3)}$$

This is ideal since HCl and Cl_2 are easily removed from the gas stream by a water spray (or bubbling). H_2 and CO_2 can be simply be vented to the atmosphere. This stoichiometry is, however, difficult to achieve with high efficiency at low gas temperatures (300 - 500 K) at which most plasmas operate. The higher gas temperature present in the MHCP will help overcome this problem.

DOE Need

SR-1017 Pollution Prevention Technologies, SR-1021 Need to Reduce the Dioxin and Furan Emissions from the CIF. ID-2.1.41 HLW Process Off-gas Treatment. ID-3.1.31.

Objectives

The objective of the project is to build and evaluate a micro hollow cathode array for the treatment of VOCs, using TCE as an example.

Work Accomplished

All major components have arrived with the exception of the power. The lack of a graduate student continues to hinder progress.

Work Planned

Assembly and testing of the system will begin, subject to time restraints and hardware delivery.

Reference

16. R. Block, et al. October 1998. Temperature Measurement in Micro Hollow Cathode Discharge in Atmospheric Air. GEO98.

Laser-induced Breakdown Spectroscopy

H. Zhang, F. Y. Yueh and J. P. Singh

Introduction

Toxic metal emissions from various waste processing off-gas systems represent a significant health hazard. This technical task has been focused on the development and application of laser-induced breakdown spectroscopy (LIBS) to monitor RCRA metals from thermal treatment processing facilities. LIBS is a laser based, nonintrusive, and sensitive optical diagnostic technique for measuring the concentration of various atomic and molecular species in test media.[17,18] It uses a high power laser beam to produce a laser-induced plasma at the test point. The plasma atomizes and electronically excites the various atomic species present in the test volume in a single step. The intensities of the atomic emission lines observed in the LIBS spectrum are used to infer the concentration of the atomic species. LIBS has successfully demonstrated its real time monitoring capability in various field tests.[19-23] The field test results also indicated that LIBS calibration techniques need further improvement to provide accurate quantitative measurement in various test environments. The LIBS calibration method has been tested with great success with laboratory data. However, practical environments are quite different from that of a laboratory. Transferring the LIBS calibration obtained in a laboratory to field measurement is a great challenge. The effects of gas stream conditions (temperature, particle size and density, etc.) on LIBS calibration has not been systematically studied. A series of

studies needs to be conducted in a simulated system to study the effects of gas stream parameters on LIBS calibration.

Work Performed

During this work period, LIBS measurements were performed in a mini combustion test stand to study the effects of gas flow and gas temperature on LIBS calibration. The setup used for the LIBS measurements is shown in Figure 16. The mini test stand is a low flow rate, bench scale combustion (50 lb/hr air max) train. It provides a flexible and well controlled environment for LIBS calibration studies. The known amounts of metal aerosol were injected in the test stand using an ultrasonic nebulizer (USN). The LIBS system was located on an optical port ~ 24 in. downstream of the inlet to the 2-in. diameter test train. Initial studies were performed on the effects of gas flow rate and temperature on LIBS calibration. Preliminary data showed a nonlinear relation between the LIBS signal and gas flow rate. Carefully repeated measurements showed the LIBS signal is inversely proportional to the gas flow rate as expected (see Figure 17). We have found the efficiency of the nebulizer (which delivers the metal aerosols to the test stand) changes with the flow rate of the gas stream. Previously, nonlinear calibration curves of Pb and Cr were found in measurements using different flow rates, which were also attributed to a nonlinear nebulizer efficiency. In the miniature test stand measurements, the injected metal aerosol is quickly diluted in the gas stream. Therefore, we injected high metal concentration solutions into the gas stream to improve the signal to noise ratio. However, the nebulizer could not efficiently deliver the metal aerosol with such a high metal solution. To avoid using the high metal solution in the planned study, we need to repeat the measurements with Be which is the most sensitive element in LIBS measurements.

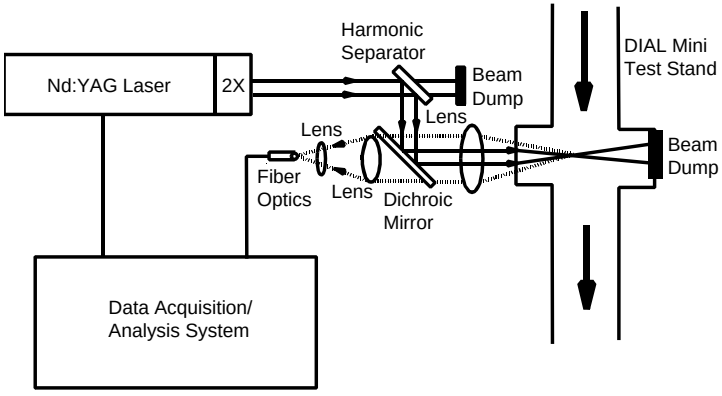

FIGURE 16. LIBS experimental setup.

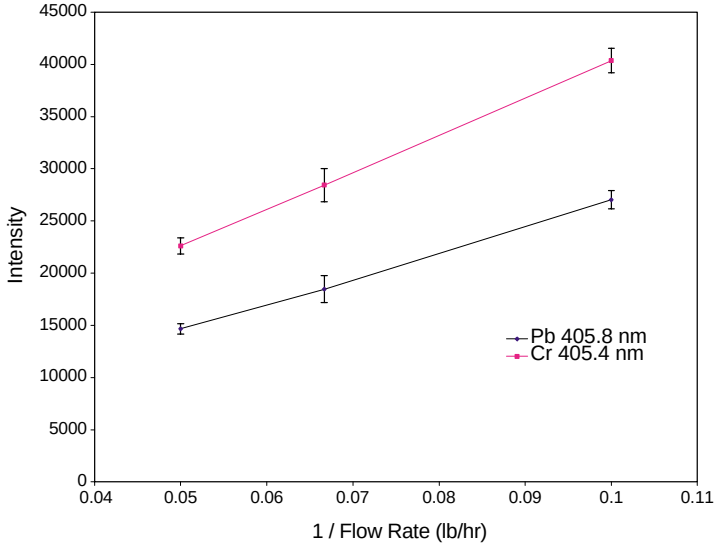

FIGURE 17. Atomic line intensity at different gas flow rates.

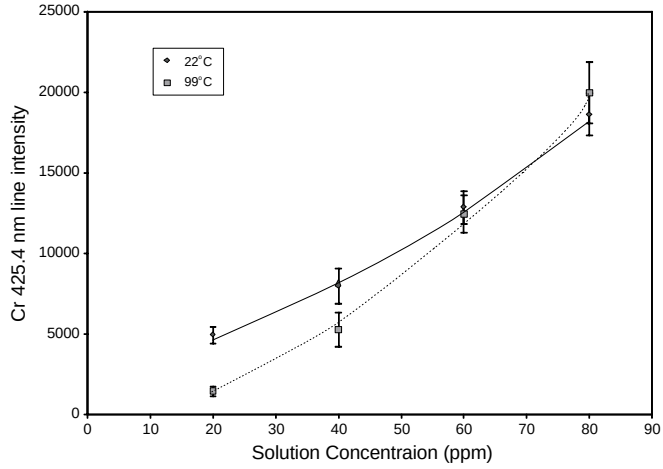

FIGURE 18. Cr calibration data at different gas temperatures.

Table 7 shows the data taken at different gas flow rates. The intensity ratios of the Pb 405.8-nm line to the Cr 425.4-nm line and the Cr 428.9-nm line to the Cr 425.4-nm line are close to a constant for different gas flow rates. This test indicates a similar plasma condition in the flow range studied. Within the gas flow rates studied here, LIBS calibration data obtained at one gas flow rate should be able to calibrate the data collected under a different gas flow rate.

TABLE 7. Atomic line intensity ratios at different gas flow rates.

Gas Flow Rate (lb/hr)	$I_{Cr\ 428.9} / I_{Cr\ 425.4}$	$I_{Pb\ 405.8} / I_{Cr\ 425.4}$
10	0.67 ± 0.004	0.584 ± 0.006
15	0.649 ± 0.015	0.597 ± 0.011
20	0.648 ± 0.005	0.578 ± 0.019

The calibration data were also collected under different gas temperatures to study the effects of gas temperature on LIBS calibration. The preheated air was mixed with the metal aerosol and sent to the

mini test stand. The gas temperature was measured at a point just downstream of the LIBS port. In this test, the air flow rate was fixed. Figure 18 shows Cr calibration data obtained at different gas temperatures. The observed nonlinear relation between the LIBS signal and solution concentration at higher temperature was suspected to be due to the nonlinear nebulizer efficiency. More studies will be performed with Be at different gas temperatures to avoid the use of a high concentration solution.

Work Planned

The study of the effects of gas stream conditions on LIBS measurements will be repeated with Be aerosol. LIBS CEM test will be conducted in the DIAL test stand. Work on design, construction and testing an all optical fiber LIBS probe for glass measurement will begin.

References

17. D.A. Cremers and L.J. Radziemski. 1987. Laser Plasmas for Chemical Analysis. *Laser Spectroscopy and its Application,* L.J. Radziemski, R.W. Solarz, J.A. Paisner, eds. New York: Marcel Dekker. Ch. 5, p.351.

18. L.J. Radziemski and D.A. Cremers. 1989. Spectrochemical Analysis Using Plasma Excitation. *Laser Induced Plasmas and Applications,* L.J. Radziemski and D.A. Cremers, eds. New York: Marcel Dekker. Ch. 7, p. 295-326.

19. J.P. Singh, F.Y. Yueh, H. Zhang. 1997. *Process control and quality.* 10:247.

20. J.P. Singh, H. Zhang, F.Y. Yueh, and K.P. Carney. 1996. *Applied Spectroscopy.* 50:764.

21. J.P. Singh, H. Zhang and F.Y. Yueh. February 1996. Transportable Vitrification System Shakedown Test, Westinghouse Savannah River Corporation and Diagnostic Instrumentation and Analysis Laboratory:

Laser-induced Breakdown Spectroscopy Measurements. US DOE Contract No. DE-FG02-93CH-10575. DIAL 10575 Trip Report 96-1.3.

22. J.P. Singh, H. Zhang and F.Y. Yueh. April 1996. DOE and EPA Continuous Emission Monitoring Test at EPA National Risk Management Research Laboratory (NRMRL). US DOE Contract No. DE-FG02-93CH-10575. DIAL 10575 Trip Report 96-2.

23. J.P. Singh, H. Zhang and F.Y. Yueh. 1996. Plasma Arc Centrifugal Treatment PACT-6 Slip Stream Test Bed (SSTB) 100-hour Duration Controlled Emission Demonstration (CED) Test. DIAL Trip Report 96-3.

24. J.P. Singh, H. Zhang and F.Y. Yueh. September 1997. DOE and EPA Continuous Emission Monitoring Test at EPA National Risk Management Research Laboratory (NRMRL), DIAL Trip Report 97-1.